

Pairwise combinations of chemical compounds that delay yeast chronological aging through different signaling pathways display synergistic effects on the extent of aging delay

Pamela Dakik¹, Mélissa McAuley¹, Marisa Chancharoen¹, Darya Mitrofanova¹, Monica Enith Lozano Rodriguez¹, Jennifer Anne Baratang Junio¹, Vicky Lutchman¹, Berly Cortes¹, Éric Simard² and Vladimir I. Titorenko¹

¹Department of Biology, Concordia University, Montreal, Quebec, Canada

²Idunn Technologies Inc., Rosemere, Quebec, Canada

Correspondence to: Vladimir I. Titorenko, **email:** vladimir.titorenko@concordia.ca

Keywords: yeast; cellular aging; geroprotectors; cellular signaling; gerotarget

Received: November 15, 2018

Accepted: December 20, 2018

Published: January 08, 2019

Copyright: Dakik et al. This is an open-access article distributed under the terms of the Creative Commons Attribution License 3.0 (CC BY 3.0), which permits unrestricted use, distribution, and reproduction in any medium, provided the original author and source are credited.

ABSTRACT

We have recently discovered six plant extracts that delay yeast chronological aging. Most of them affect different nodes, edges and modules of an evolutionarily conserved network of longevity regulation that integrates certain signaling pathways and protein kinases; this network is also under control of such aging-delaying chemical compounds as spermidine and resveratrol. We have previously shown that, if a strain carrying an aging-delaying single-gene mutation affecting a certain node, edge or module of the network is exposed to some of the six plant extracts, the mutation and the plant extract enhance aging-delaying efficiencies of each other so that their combination has a synergistic effect on the extent of aging delay. We therefore hypothesized that a pairwise combination of two aging-delaying plant extracts or a combination of one of these plant extracts and spermidine or resveratrol may have a synergistic effect on the extent of aging delay only if each component of this combination targets a different element of the network. To test our hypothesis, we assessed longevity-extending efficiencies of all possible pairwise combinations of the six plant extracts or of one of them and spermidine or resveratrol in chronologically aging yeast. In support of our hypothesis, we show that only pairwise combinations of naturally-occurring chemical compounds that slow aging through different nodes, edges and modules of the network delay aging in a synergistic manner.

INTRODUCTION

Different patient-customized combinations of Chinese plants have been for centuries used in traditional Chinese herbal medicine to prevent and treat a wide range of human diseases [1–4]. The recent use of high-throughput “omics”, system biological and bioinformatic approaches in animal models of many human diseases and in cultured human cells has revealed that these combinations of Chinese plants affect multiple cellular and organismal processes [4, 5–8]. The term “network pharmacology” (also known as “Traditional Chinese

Medicine [TCM] network pharmacology”) has been introduced to describe such systemic effects of various combinations of Chinese herbs on the cellular and organismal networks integrating multiple disease-related processes [9–19]. The key tenet of the TCM network pharmacology concept is that the high therapeutic effectiveness, multitude of targeted pathologies and limited side effects of Chinese herbal medicine are due to the ability of cocktails of plant chemical compounds to affect multiple molecular targets through numerous low-affinity interactions [4, 9–22]. A body of evidence supports the notion that, by modulating different nodes, edges and

modules of these disease-specific networks, a combined action of Chinese herb mixtures allows to restore cellular and organismal homeostasis differently altered in diverse human diseases [4, 8, 15, 19–22].

The two important conceptual advances in our understanding of the biology of human diseases are the following: 1) many (in not all) human diseases are due to various perturbations in complex networks that assimilate specific signaling, metabolic and other molecular pathways; and 2) a rational design of certain combinations of pure drugs and/or natural chemical compounds, each targeting different nodes, edges or modules of such networks, may yield potent multicomponent therapies with limited side effects and lowered potential of drug resistance development [23–36]. A development of such multicomponent therapies with the help of high-throughput screening methods for identifying effective combinations of therapeutic compounds represents an essential strategy of modern medicine [23–37]. This strategy has been successfully used for the development of multicomponent and multitargeted therapeutics for the treatment of complex human diseases, including cancer, infectious diseases, central nervous system disorders, Alzheimer's disease, hypertension, chronic obstructive pulmonary disease, asthma and acquired immunodeficiency syndrome [23, 32, 34, 35, 37–49]. The significant progress in developing multicomponent and multitargeted therapeutics has been facilitated by the advances in mathematical, computational and pharmacological approaches to study compound combination effects [37, 49–58].

Incidence rates of many human chronic diseases increase with age [59–63]. Because an age-related dysregulation of certain cellular and organismal processes is the primary cause of these chronic diseases, they are considered as diseases associated with aging [60, 61, 64–66]. Among these aging-associated human diseases are cardiovascular diseases, chronic obstructive pulmonary disease, chronic kidney disease, diabetes, osteoarthritis, osteoporosis, sarcopenia, stroke, neurodegenerative diseases (including Parkinson's, Alzheimer's and Huntington's diseases), and many forms of cancer [61–70]. The major aspects and basic mechanisms of aging and aging-associated pathology have been conserved over the course of evolution; they include the following: 1) the hallmark events of aging, such as the age-related accumulation of genomic damage, deterioration of telomeres, epigenetic perturbations, impairment of cellular proteostasis, deregulation of nutrient-sensing systems, decline in mitochondrial functionality, accumulation of senescent cells, decrease of the abundance and functionality of stem cells, and deterioration of intercellular communications [68]; 2) the nutrient- and energy-sensing signaling network of longevity regulation, which integrates the insulin/insulin-like growth factor 1 (IGF-1) pathway, AMP-activated protein kinase/target of rapamycin (AMPK/TOR) pathway, cAMP/protein kinase

A (cAMP/PKA) pathway and sirtuin-governed protein deacetylation module [66–68, 71–73].

Some of the known hallmarks of aging and signaling pathways of longevity regulation are specifically targeted by certain individually added chemical compounds (either synthetic drugs or natural chemicals) that delay the onset and decelerate the progression of the aging process in eukaryotes across phyla [60, 64–70, 74–76]. It needs to be emphasized that none of these individually added aging-delaying chemical compounds can affect all hallmarks of aging or modulate all signaling pathways of longevity regulation [64–67, 75, 76]. It has been therefore proposed that, if two or more aging-delaying chemical compounds each targeting a different hallmark and/or signaling pathway of aging are added together, their combination may have an additive or a synergistic effect on the extent of aging delay and longevity extension [74–77]. The following multicomponent combinations of chemical compounds have been proposed for such therapeutic multiplexing of aging delay and longevity extension: 1) a three-component mixture of epigallocatechin gallate (an activator of cAMP synthesis), N-acetyl-L-cysteine (an inhibitor of cell proliferation pathways) and myricetin (an activator of integrin signaling, DNA repair, cAMP synthesis and hypoxia signaling) [74]; 2) a seven-component mixture of rapalogs (including rapamycin and its synthetic drug analogs, all of which are inhibitors of the pro-aging TOR pathway), metformin (an activator of AMPK, which is a major cellular regulator of glucose and lipid metabolism), losartan or lisinopril (both of which are inhibitors of angiotensin II signaling), a statin (such as atorvastatin, simvastatin or lovastatin, all of which decrease blood cholesterol levels), propranolol (a non-cardioselective beta-adrenergic antagonist), aspirin (an inhibitor of cyclooxygenase) and a phosphodiesterase 5 inhibitor, in combination with physical exercise and caloric restriction (CR) diet or intermittent fasting [76, 78]; and 3) a three-component mixture of rapamycin, acarbose (an α-glucosidase inhibitor) and a cardiolipin-binding peptide [77].

Recent studies in mice have supported the notion that a combination of the aging-delaying chemical compounds that target different aging-associated processes may exhibit a synergistic effect on the extent of aging delay; this combination included rapamycin and metformin [79, 80]. This notion has also been supported by the following studies in model eukaryotic organisms: 1) pairwise combinations of rapamycin and wortmannin (an inhibitor of phosphoinositide 3-kinase), rapamycin and pyrrolidine dithiocarbamates (PDTC; inhibitors of the NF-κB pathway), and wortmannin and PDTC have been shown to exhibit synergistic effects on the extent of *Drosophila melanogaster* lifespan extension [81]; 2) a pairwise combination of rapamycin and an inhibitor of the stress-activated c-Jun N-terminal kinase have been demonstrated to act in synergy to prolong longevity of the coastal marine and salt-lake rotifer *Brachionus manjavacas* [82]; 3) some double and triple combinations of synthetic drugs

and natural chemicals that target the IGF-1, transforming growth factor β and sterol regulatory element-binding protein signaling pathways of longevity regulation have been shown to extend the lifespan of the nematode *Caenorhabditis elegans* in a synergistic manner [83]; and 4) rapamycin and myriocin (an inhibitor of sphingolipid synthesis) act in synergy to extend chronological lifespan in the budding yeast *Saccharomyces cerevisiae* and in the fission yeast *Schizosaccharomyces pombe* [84, 85].

Our recent study has revealed six plant extracts (PEs) that significantly extend the chronological lifespan (CLS) of the yeast *S. cerevisiae* under non-CR conditions [86]. We called them PE4 (an extract from the root and rhizome of *Cimicifuga racemosa*), PE5 (an extract from the root of *Valeriana officinalis L.*), PE6 (an extract from the whole plant of *Passiflora incarnata L.*), PE8 (an extract from the leaf of *Ginkgo biloba*), PE12 (an extract from the seed of *Apium graveolens L.*) and PE21 (an extract from the bark of *Salix alba*) [86]. These six longevity-extending PEs are geroprotectors that postpone the onset and decelerate the progression of yeast chronological aging; each of them promotes a hormetic stress response and exhibits a different effect on a distinct set of longevity-defining cellular processes [86]. We have also demonstrated that PE4, PE5, PE6, PE8, PE12 and PE21 delay yeast chronological aging via an evolutionarily conserved network of signaling pathways and protein kinases (Supplementary Figure 1) [87]. Most of the six PEs slows down aging by modulating different nodes, edges and modules of this intricate network of longevity regulation (Supplementary Figure 1) [87]; some of these elements of the network are also under control of such naturally-occurring aging-delaying chemical compounds as spermidine and resveratrol (Supplementary Figure 1) [64, 67, 88–94]. We noticed that, if a strain carrying an aging-delaying single-gene mutation affecting a certain node, edge or module of the network is exposed to some of the six PEs, the mutation and the PE enhance aging-delaying efficiencies of each other so that their combination has a synergistic effect on the extent of aging delay [87]. Based on these observations, we hypothesized that a pairwise combination of two aging-delaying PEs or a combination of one of these PEs and spermidine or resveratrol may exhibit a synergistic effect on the extent of aging delay only if each of the two components of this combination targets a different node, edge or module of the network. This study is a proof-of-concept investigation aimed at testing our hypothesis by a systematic assessment of longevity-extending efficiencies of all possible pairwise combinations of PE4, PE5, PE6, PE8, PE12 and PE21 or of one of these PEs and spermidine or resveratrol in chronologically aging yeast. In support of our hypothesis, we show that only pairwise combinations of naturally-occurring chemical compounds that delay yeast chronological aging through different nodes, edges and modules of the longevity regulation network display

synergistic effects on the extent of aging delay. Because investigations in *S. cerevisiae* have previously provided evidence that the major aspects and basic mechanisms of aging and aging-associated pathology are evolutionarily conserved [64, 67, 88, 91, 94–102], this study advances our knowledge of how multicomponent combinations of natural chemical compounds can be used for therapeutic multiplexing of aging delay and longevity extension.

RESULTS

Our hypothesis on possible synergistic longevity-extending effects of certain pairwise combinations of the six aging-delaying PEs and/or spermidine and resveratrol

A signaling network that controls the rate of yeast chronological aging is schematically depicted in Supplementary Figure 1. This network integrates the following signaling pathways and protein kinases: 1) the pro-aging TORC1 (target of rapamycin complex 1) pathway; 2) the pro-aging PKA (protein kinase A) pathway; 3) the pro-aging PKH1/2 (Pkb-activating kinase homolog) pathway; 4) the anti-aging SNF1 (sucrose non-fermenting) pathway; 5) the anti-aging ATG (autophagy) pathway; 6) the pro-aging protein kinase Sch9, which is activated by the TORC1 and PKH1/2 pathways; and 7) the anti-aging protein kinase Rim15, which is suppressed by the TORC1, PKA and PKH1/2 pathways (Supplementary Figure 1) [67, 87, 96, 97, 103–107]. The network modulates such longevity-defining cellular processes as gluconeogenesis, glyoxylate cycle, glycogen synthesis and degradation, amino acids synthesis, fatty acids synthesis, mitochondrial respiration, protein synthesis in the cytosol and mitochondria, maintenance of nuclear and mitochondrial genomes, peroxisome biogenesis, autophagy, and stress responses (Supplementary Figure 1) [67, 96, 97, 105–117]. PE4, PE5, PE6, PE8, PE12 and PE21 delay yeast chronological aging because they elicit the following effects on different nodes, edges and modules of the network: 1) PE4 lessens the inhibitory action of the pro-aging TORC1 pathway on the anti-aging SNF1 pathway; 2) PE5 suppresses two different branches of the pro-aging PKA pathway; 3) PE6 regulates cellular processes that are not integrated into the network; 4) PE8 inhibits the suppressive effect of PKA on SNF1; 5) PE12 stimulates the anti-aging protein kinase Rim15; and 6) PE21 downregulates a form of the pro-aging protein kinase Sch9 that is stimulated by the pro-aging PKH1/2 pathway (Supplementary Figure 1) [87].

It has previously demonstrated that spermidine, a polyamine of plant origin, delays the chronological mode of aging in yeast and other organisms by activating the anti-aging ATG1 (autophagy) pathway (Supplementary Figure 1) [88, 89, 92, 97, 100]. Moreover, although resveratrol has been shown to extend

mammalian healthspan by suppressing cAMP-dependent phosphodiesterases to elicit AMPK activation [118] and by stimulating the tyrosyl transfer-RNA synthetase to promote poly(ADP-ribose) polymerase 1 auto-poly-ADP-ribosylation [119], the molecular targets of this plant phenolic compound in chronologically aging yeast remain unknown (Supplementary Figure 1).

As we have already mentioned, the following two observations provide the basis for our hypothesis: 1) most of the six aging-delaying PEs, as well as spermidine and resveratrol, modulate different nodes, edges and modules of the signaling network that controls the rate of yeast chronological aging (Supplementary Figure 1) [87]; the only possible exception is the demonstrated abilities of PE4 and PE8 to weaken the restraining action of two different network's edges (i.e. the pro-aging TORC1 pathway and PKA pathway, respectively) on the same node (i.e. the anti-aging SNF1 pathway) of the network (Supplementary Figure 1) [87]; and 2) certain combinations of one of the six PEs and aging-delaying single-gene mutations that affect these nodes, edges and modules display synergistic effects on the extent of yeast chronological aging delay [87]. We therefore put forward the hypothesis that most of 27 possible pairwise combinations of two aging-delaying PEs or of one of these PEs and spermidine or resveratrol (Supplementary Table 1) may slow down yeast chronological aging in a synergistic manner. We also hypothesized that a combination of PE4 and PE8 may not display a synergistic effect on the extent of yeast chronological aging delay. To test these hypotheses, we assessed longevity-extending efficiencies of all possible pairwise combinations of PE4, PE5, PE6, PE8, PE12 and PE21 or of one of these PEs and spermidine or resveratrol in chronologically aging yeast.

An effect-based model that we used to assess if a pairwise combination of aging-delaying chemical compounds has a synergistic effect on the extent of aging delay

Several effect-based models have been developed to assess if a pairwise combination of chemical compounds exhibits a synergistic effect on the monitored process, i.e. if the positive effect of this combination on the process exceeds the positive effects of individual compounds comprising the combination [23, 28, 29, 50, 56, 120–123]. In this study, we have used the highest single agent (HSA) model for evaluating if two PEs or a PE and spermidine or resveratrol extend yeast longevity synergistically if used in a pairwise combination; this model has been recently used to demonstrate that certain drug combinations have synergistic effects on aging delay and healthspan extension in the nematode *C. elegans* [83]. According to the HSA model, two chemical compounds are considered to act in synergy if the effect of their combination exceeds the effect of a component of this combination that exhibits the

highest effect if it is used alone [50, 56, 120, 123]. Using the HSA model, we have calculated the Combination Index (CI) value (which is considered as the standard measure of combination effect [50, 56, 120, 123]) as follows: $CI = \text{CLS}_X/\text{CLS}_{X+Y}$ (if chemical compound X is the HSA) or $CI = \text{CLS}_Y/\text{CLS}_{X+Y}$ (if chemical compound Y is the HSA) for both the mean and maximum CLS of yeast exposed to compound X alone, to compound Y alone or to a mixture of compounds X and Y. We have calculated the significance of a synergistic effect (i.e. $CI < 1$) as the *p* value of the two-tailed *t* test for comparing the effect of a combination of chemical compounds (i.e. CLS_{X+Y}) to that of the HSA (i.e. CLS_X or CLS_Y for the mean and maximum CLS).

Mixtures of PE4 and PE5, PE4 and PE6, PE4 and PE12, and PE4 and PE21 have synergistic effects on the extent of aging delay

PE4, PE5, PE6, PE12 or PE21 have been shown to modulate different nodes, edges and modules of the signaling network that controls the rate of yeast chronological aging [87]. Specifically, these PEs delay aging as follows: 1) PE4 weakens the restraining action of the pro-aging TORC1 pathway on the anti-aging SNF1 pathway; 2) PE5 mitigates two different branches of the pro-aging PKA pathway; 3) PE6 modulates a presently unknown pro-aging or anti-aging node that may be integrated into this network; 4) PE12 stimulates the anti-aging protein kinase Rim15; and 5) PE21 inhibits a form of the pro-aging protein kinase Sch9 that is activated by the pro-aging PKH1/2 pathway (Supplementary Figure 1) [87]. We therefore hypothesized that mixtures of PE4 with PE5, PE6, PE12 or PE21 may exhibit synergistic effects on the extent of yeast chronological aging delay. To test this hypothesis, we cultured wild-type (WT) cells in the synthetic minimal medium initially containing 2% glucose, either without a PE (i.e. cells were subjected to ethanol-mock treatment) or with the following additions: 1) PE4, PE5, PE6, PE12 or PE21 alone (each being used at the final concentration of 0.1%, 0.5% or 1.0%, see below); or 2) a mixture of 0.1%, 0.3%, 0.5% or 1.0% PE4 with PE5, PE6, PE12 or PE21 (each being used at the final concentration of 0.1%, 0.3%, 0.5% or 1.0%).

We found that the longevity-extending efficiencies of the following pairwise combinations of aging-delaying PEs statistically significantly exceed that of a PE within the pair which was considered as the HSA if this PE was used alone at the optimal aging-delaying concentration: 1) a mixture of 0.3% PE4 and 0.3% PE5 (if PE4 and PE5 were used at these final concentrations, their mixture exhibited the highest longevity-extending effect) as compared to 0.5% PE4 (which was used as the HSA for both the mean and maximum CLS), with $CI = 0.63$ for the mean CLS and $CI = 0.56$ for the maximum CLS (Figure 1); 2) a mixture of 0.5% PE4 and 1.0% PE6 as compared to

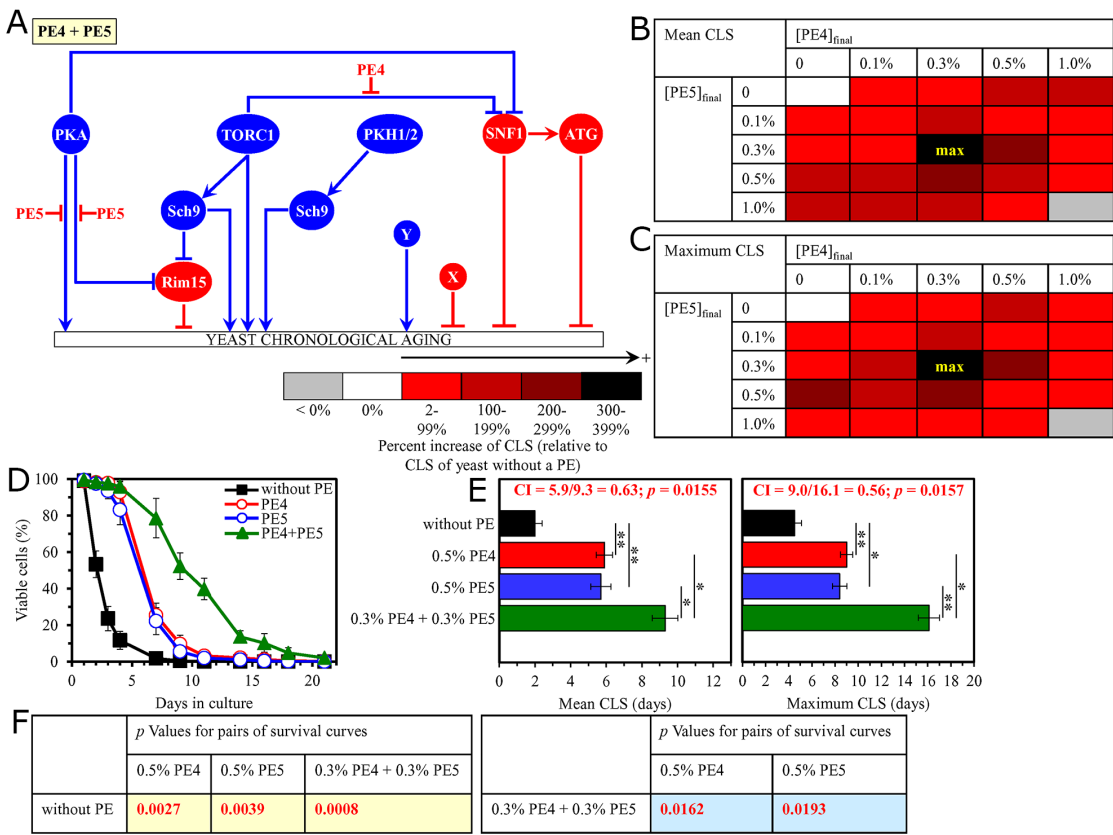


Figure 1: The longevity-extending efficiency of a mixture of 0.3% PE4 and 0.3% PE5 statistically significantly exceeds those of PE4 and PE5, each being used at the optimal concentration of 0.5%. Thus, PE4 and PE5 enhance the longevity-extending efficiency of each other. Hence, according to the highest single agent (HSA) model, PE4 and PE5 act in synergy to extend longevity of chronologically aging yeast. (A) PE4 and PE5 are known to inhibit different pro-aging nodes of the signaling network that controls the rate of yeast chronological aging. PE4 weakens the restraining action of the pro-aging TORC1 pathway on the anti-aging SNF1 pathway, whereas PE5 mitigates two different branches of the pro-aging PKA pathway. (B, C) Wild-type (WT) cells were grown in the synthetic minimal YNB medium initially containing 2% glucose, with PE4 and/or PE5 (at the final concentration of 0.1%, 0.3%, 0.5% or 1.0%) or without a PE. Effects of different concentrations of PE4 and PE5 (added alone or in pairwise combinations) on the mean (B) or maximum (C) chronological lifespan (CLS) of WT cells are shown. The table cell at the intersection of the column for 0.3% PE4 and the row for 0.3% PE5 is marked "max" because the mixture of 0.3% PE4 and 0.3% PE5 exhibits the highest extending effect on the mean and maximum lifespans of chronologically aging WT cells. (D, E) WT cells were cultured in the synthetic minimal YNB medium initially containing 2% glucose and one of the following supplements: 0.5% PE4, 0.5% PE5, or a mixture of 0.3% PE4 and 0.3% PE5. In the cultures supplemented with PE4 and/or PE5, ethanol was used as a vehicle at the final concentration of 2.5%. In the same experiment, WT cells were also subjected to ethanol-mock treatment by being cultured in the synthetic minimal YNB medium initially containing 2% glucose and 2.5% ethanol. Survival curves (D) and the mean and maximum lifespans (E) of chronologically aging WT cells cultured without a PE (cells were subjected to ethanol-mock treatment), with 0.5% PE4, with 0.5% PE5, or with the mixture of 0.3% PE4 and 0.3% PE5 are shown. Data in D and E are presented as means \pm SEM ($n = 3$; * $p < 0.05$; ** $p < 0.01$). The Combination Index (CI) values in E were calculated as follows: $CI = \text{CLS}_{\text{PE4}}/\text{CLS}_{\text{PE4+PE5}}$ for both the mean and maximum CLS; the significance of a synergistic effect (i.e. $CI < 1$) is provided as the p value of the two-tailed t test for comparing the effect of a PE combination (i.e. $\text{CLS}_{\text{PE4+PE5}}$) to that of the HSA (i.e. CLS_{PE4} for both the mean and maximum CLS). Data for mock-treated WT cells are replicated in graphs D and E of Figures 2–14 and Supplementary Figures 2–14. Data for WT cells cultured with 0.5% PE4 are replicated in graphs D and E of Figures 2–4, Figure 11, Supplementary Figure 2 and Supplementary Figure 9. Data for WT cells cultured with 0.5% PE5 are replicated in graphs D and E of Figure 5, Figure 6, Figure 9, Supplementary Figure 3 and Supplementary Figure 4. (F) p Values for different pairs of survival curves of WT cells cultured in the presence of 0.5% PE4, 0.5% PE5, a mixture of 0.3% PE4 and 0.3% PE5, or in the absence of a PE (cells were subjected to ethanol-mock treatment) are shown. Survival curves shown in (D) were compared. Two survival curves were considered statistically different if the p value was less than 0.05. The p values for comparing pairs of survival curves using the logrank test were calculated as described in Materials and Methods. The p values displayed on a yellow color background indicate that 0.5% PE4, 0.5% PE5, and the mixture of 0.3% PE4 and 0.3% PE5 significantly extend the CLS of WT cells. The p values displayed on a blue color background indicate that the CLS-extending efficiency of the mixture of 0.3% PE4 and 0.3% PE5 significantly exceeds that of 0.5% PE4 or 0.5% PE5. Abbreviations: ATG, autophagy; PKA, protein kinase A; PKH1/2, Pkb-activating kinase homologs 1 and 2; Rim15, an anti-aging protein kinase; Sch9, a pro-aging protein kinase; SNF1, sucrose non-fermenting protein 1; TORC1, target of rapamycin complex 1; X, a presently unknown anti-aging node of this signaling network; Y, a presently unknown pro-aging node of this signaling network.

0.5% PE4 (which was used as the HSA for both the mean and maximum CLS) (Supplementary Figure 2); 3) a mixture of 0.5% PE4 and 0.1% PE12 as compared to 0.5% PE4 (which was used as the HSA for the mean CLS) or 0.1% PE12 (which was used as the HSA for the

maximum CLS) (Figure 3); and 4) a mixture of 0.5% PE4 and 0.1% PE21 as compared to 0.1% PE21 (which was used as the HSA for both the mean and maximum CLS), with CI = 0.61 for the mean CLS and CI = 0.73 for the maximum CLS (Figure 4).

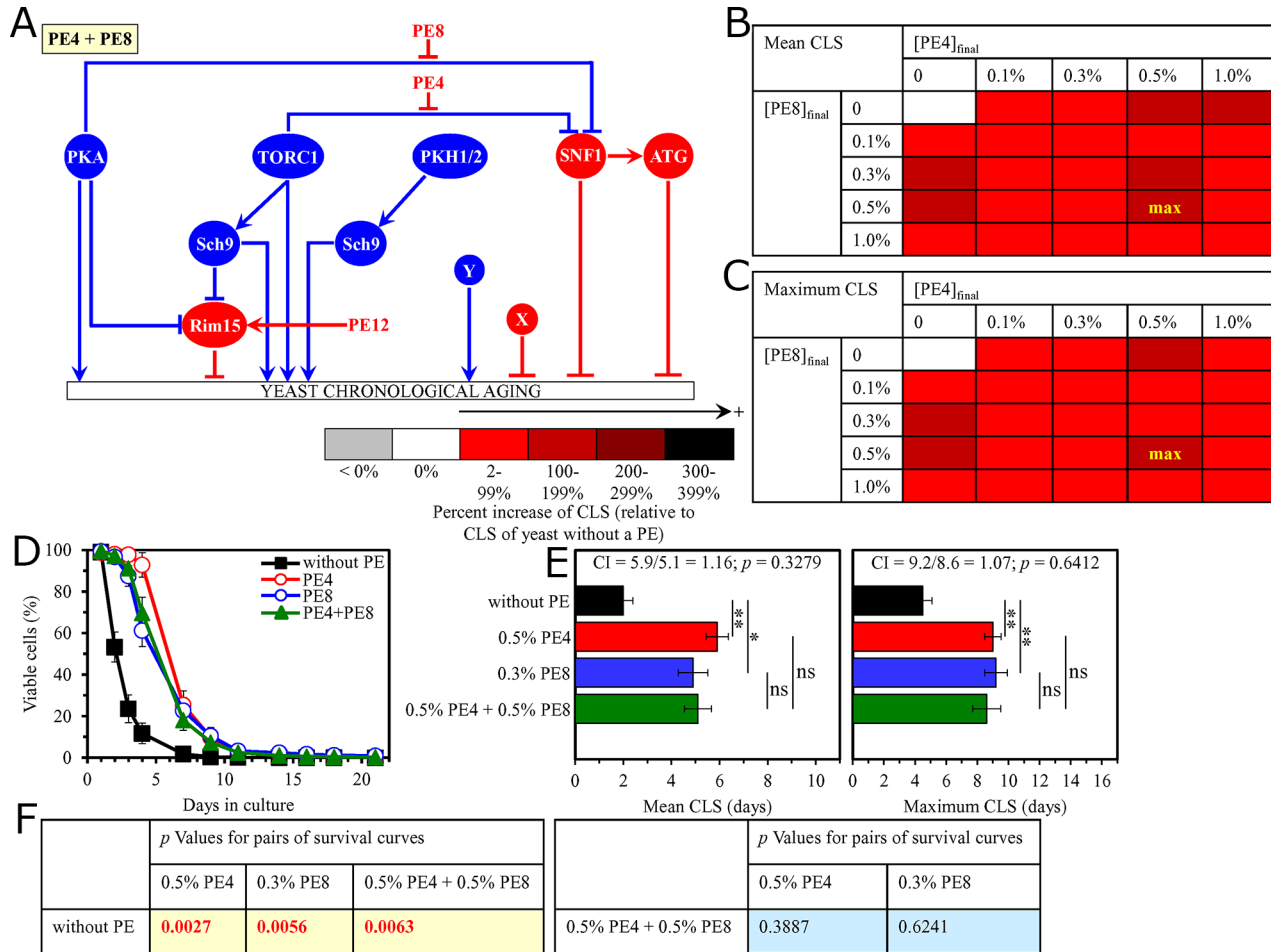


Figure 2: The longevity-extending efficiency of a mixture of 0.5% PE4 and 0.5% PE8 is not statistically different from those of PE4 and PE8, which were used at the optimal concentration of 0.5% or 0.3% (respectively). Thus, PE4 and PE8 do not enhance the longevity-extending efficiency of each other. Hence, according to the HSA model, PE4 and PE8 do not act in synergy to extend longevity of chronologically aging yeast. **(A)** PE4 and PE8 are known to weaken the restraining action of the pro-aging TORC1 or PKA pathway on the same node (i.e. the anti-aging SNF1 pathway) of the signaling network that controls the rate of yeast chronological aging. **(B, C)** WT cells were grown as described in the legend to Figure 1, with PE4 and/or PE8 (at the final concentration of 0.1%, 0.3%, 0.5% or 1.0%) or without a PE. Effects of different concentrations of PE4 and PE8 (added alone or in pairwise combinations) on the mean (B) or maximum (C) CLS of WT cells are shown. The table cell at the intersection of the column for 0.5% PE4 and the row for 0.5% PE8 is marked "max" for the reason described in the legend to Figure 1. **(D, E)** WT cells were cultured as described in the legend to Figure 1, with one of the following supplements: 0.5% PE4, 0.3% PE8, or a mixture of 0.5% PE4 and 0.5% PE8. Ethanol was used as a vehicle or for mock treatment as described in the legend to Figure 1. Survival curves (D) and the mean and maximum lifespans (E) of chronologically aging WT cells cultured without a PE (cells were subjected to ethanol-mock treatment), with 0.5% PE4, with 0.3% PE8, or with the mixture of 0.5% PE4 and 0.5% PE8 are shown. Data in D and E are presented as means \pm SEM ($n = 3$; * $p < 0.05$; ** $p < 0.01$). The CI and p values in E were calculated as described in the legend to Figure 1. Data for mock-treated WT cells are replicated in graphs D and E of Figure 1, Figures 3–14 and Supplementary Figures 2–14. Data for WT cells cultured with 0.5% PE4 are replicated in graphs D and E of Figure 1, Figure 3, Figure 4, Figure 11, Supplementary Figure 2 and Supplementary Figure 9. Data for WT cells cultured with 0.3% PE8 are replicated in graphs D and E of Figure 5, Figure 8, Figure 10, Supplementary Figure 5, Supplementary Figure 7 and Supplementary Figure 14. **(F)** p Values for different pairs of survival curves of WT cells cultured in the presence of 0.5% PE4, 0.3% PE8, a mixture of 0.5% PE4 and 0.5% PE8, or in the absence of a PE (cells were subjected to ethanol-mock treatment) are shown. Survival curves shown in (D) were compared. Abbreviations: as in the legend to Figure 1.

In sum, these findings confirm our hypothesis that mixtures of PE4 with PE5, PE6, PE12 or PE21 slow down yeast chronological aging in a synergistic manner.

A mixture of PE4 and PE8 does not slow down yeast chronological aging in a synergistic manner

PE4 and PE8 have been shown to weaken the restraining action of the pro-aging TORC1 or PKA pathway

on the same node (i.e. the anti-aging SNF1 pathway) of the signaling network that controls the rate of yeast chronological aging (Supplementary Figure 1) [87]. We therefore hypothesized that PE4 and PE8 may not act in synergy to delay yeast chronological aging. To test this hypothesis, we cultured WT cells in the synthetic minimal medium initially containing 2% glucose, either without a PE (i.e. cells were subjected to ethanol-mock treatment) or with the following additions: 1) 0.5% PE4 or 0.3% PE8 alone (if PE4 or PE8

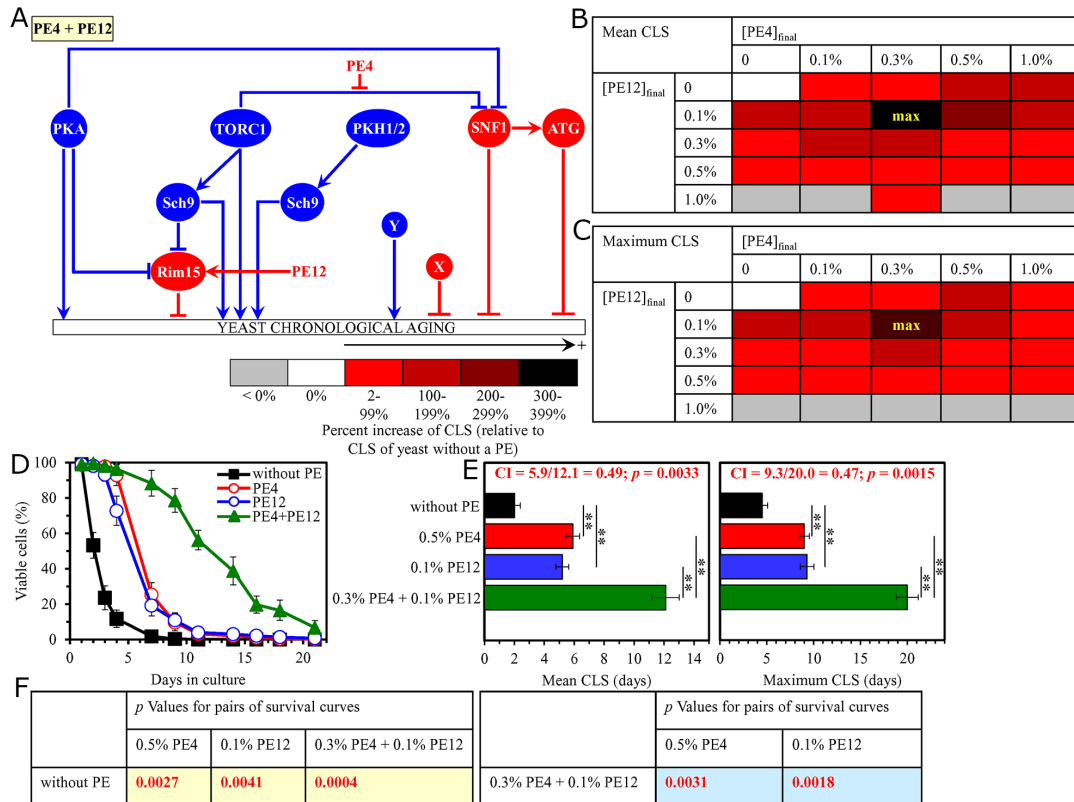


Figure 3: The longevity-extending efficiency of a mixture of 0.3% PE4 and 0.1% PE12 statistically significantly exceeds those of PE4 and PE12, which were used at the optimal concentration of 0.5% or 0.1% (respectively). Thus, PE4 and PE12 enhance the longevity-extending efficiency of each other. Hence, according to the HSA model, PE4 and PE12 act in synergy to extend longevity of chronologically aging yeast. **(A)** PE4 and PE12 are known to inhibit different pro-aging nodes of the signaling network that controls the rate of yeast chronological aging. PE4 weakens the restraining action of the pro-aging TORC1 pathway on the anti-aging SNF1 pathway, whereas PE12 stimulates the anti-aging protein kinase Rim15. **(B, C)** WT cells were grown as described in the legend to Figure 1, with PE4 and/or PE12 (at the final concentration of 0.1%, 0.3%, 0.5% or 1.0%) or without a PE. Effects of different concentrations of PE4 and PE12 (added alone or in pairwise combinations) on the mean (B) or maximum (C) CLS of WT cells are shown. The table cell at the intersection of the column for 0.3% PE4 and the row for 0.1% PE12 is marked "max" for the reason described in the legend to Figure 1. **(D, E)** WT cells were cultured as described in the legend to Figure 1, with one of the following supplements: 0.5% PE4, 0.1% PE12, or a mixture of 0.3% PE4 and 0.1% PE12. Ethanol was used as a vehicle or for mock treatment as described in the legend to Figure 1. Survival curves (D) and the mean and maximum lifespans (E) of chronologically aging WT cells cultured without a PE (cells were subjected to ethanol-mock treatment), with 0.5% PE4, with 0.1% PE12, or with the mixture of 0.3% PE4 and 0.1% PE12 are shown. Data in D and E are presented as means \pm SEM ($n = 3$; * $p < 0.05$; ** $p < 0.01$). The CI and p values in E were calculated as described in the legend to Figure 1. Data for mock-treated WT cells are replicated in graphs D and E of Figure 1, Figure 2, Figures 4–14 and Supplementary Figures 2–14. Data for WT cells cultured with 0.5% PE4 are replicated in graphs D and E of Figure 1, Figure 2, Figure 4, Figure 11, Supplementary Figure 2 and Supplementary Figure 9. Data for WT cells cultured with 0.1% PE12 are replicated in graphs D and E of Figure 7, Figure 8, Figure 13, Supplementary Figure 4, Supplementary Figure 8 and Supplementary Figure 11. **(F)** p Values for different pairs of survival curves of WT cells cultured in the presence of 0.5% PE4, 0.1% PE12, a mixture of 0.3% PE4 and 0.1% PE12, or in the absence of a PE (cells were subjected to ethanol-mock treatment) are shown. Survival curves shown in (D) were compared. The p values are displayed on a yellow or blue color background for the reasons described in the legend to Figure 1. Abbreviations: as in the legend to Figure 1.

was used at this final concentration, it exhibited the highest longevity-extending effect); or 2) a mixture of 0.1%, 0.3%, 0.5% or 1.0% PE4 with 0.1%, 0.3%, 0.5% or 1.0% PE8.

In support of our hypothesis, we found that the longevity-extending efficiency of a mixture of 0.5% PE4 and 0.5% PE8 is not statistically different from

those of PE4 and PE8, which were used at the optimal concentration of 0.5% or 0.3% (respectively) (Figure 2). The CI values were 1.16 and 1.07 for the mean CLS and the maximum CLS (respectively) when 0.5% PE4 was used as the HSA for the mean CLS and 0.3% PE8 was used as the HSA for the maximum CLS (Figure 2).

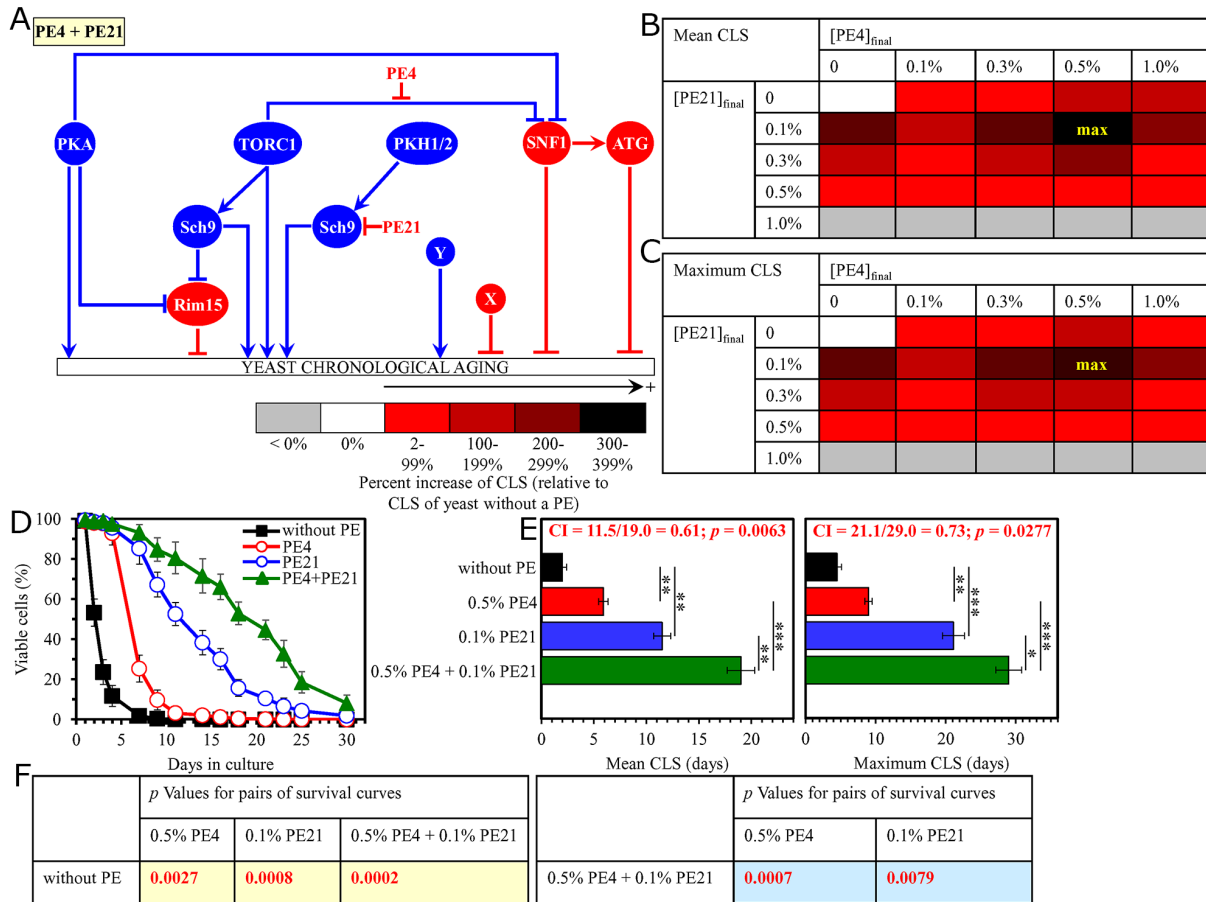


Figure 4: The longevity-extending efficiency of a mixture of 0.5% PE4 and 0.1% PE21 statistically significantly exceeds those of PE4 and PE21, which were used at the optimal concentration of 0.5% or 0.1% (respectively). Thus, PE4 and PE21 enhance the longevity-extending efficiency of each other. Hence, according to the HSA model, PE4 and PE21 act in synergy to extend longevity of chronologically aging yeast. **(A)** PE4 and PE21 are known to inhibit different pro-aging nodes of the signaling network that controls the rate of yeast chronological aging. PE4 weakens the restraining action of the pro-aging TORC1 pathway on the anti-aging SNF1 pathway, whereas PE21 mitigates a form of the pro-aging protein kinase Sch9 that is activated by the pro-aging PKH1/2 pathway. **(B, C)** WT cells were grown as described in the legend to Figure 1, with PE4 and/or PE21 (at the final concentration of 0.1%, 0.3%, 0.5% or 1.0%) or without a PE. Effects of different concentrations of PE4 and PE21 (added alone or in pairwise combinations) on the mean (B) or maximum (C) CLS of WT cells are shown. The table cell at the intersection of the column for 0.5% PE4 and the row for 0.1% PE21 is marked "max" for the reason described in the legend to Figure 1. **(D, E)** WT cells were cultured as described in the legend to Figure 1, with one of the following supplements: 0.5% PE4, 0.1% PE21, or a mixture of 0.5% PE4 and 0.1% PE21. Ethanol was used as a vehicle or for mock treatment as described in the legend to Figure 1. Survival curves (D) and the mean and maximum lifespans (E) of chronologically aging WT cells cultured without a PE (cells were subjected to ethanol-mock treatment), with 0.5% PE4, with 0.1% PE21, or with the mixture of 0.5% PE4 and 0.1% PE21 are shown. Data in D and E are presented as means \pm SEM ($n = 3$; * $p < 0.05$; ** $p < 0.01$; *** $p < 0.001$). The CI and p values in E were calculated as described in the legend to Figure 1. Data for mock-treated WT cells are replicated in graphs D and E of Figures 1–3, Figure 5, Figures 6–14 and Supplementary Figures 2–14. Data for WT cells cultured with 0.5% PE4 are replicated in graphs D and E of Figures 1–3, Figure 11, Supplementary Figure 2 and Supplementary Figure 9. Data for WT cells cultured with 0.1% PE21 are replicated in graphs D and E of Figure 6, Figure 14, Supplementary Figures 6–8 and Supplementary Figure 12. **(F)** p Values for different pairs of survival curves of WT cells cultured in the presence of 0.5% PE4, 0.1% PE21, a mixture of 0.5% PE4 and 0.1% PE21, or in the absence of a PE (cells were subjected to ethanol-mock treatment) are shown. Survival curves shown in (D) were compared. The p values are displayed on a yellow or blue color background for the reasons described in the legend to Figure 1. Abbreviations: as in the legend to Figure 1.

Pairwise combinations of PE5 and PE6, PE5 and PE8, PE5 and PE12, and PE5 and PE21 delay yeast chronological aging in a synergistic fashion

As we have already mentioned, PE5, PE6, PE8, PE12 and PE21 are known to affect different nodes, edges and modules of the signaling network that controls the rate of yeast chronological aging (Supplementary Figure 1) [87]. We therefore put forward the hypothesis that pairwise combinations of PE5 and PE6, PE5 and PE8, PE5 and PE12, and PE5 and PE21 may synergistically extend longevity of chronologically aging yeast. To test this hypothesis, WT cells were cultured in the synthetic minimal medium initially containing 2% glucose, either without a PE (i.e. cells were subjected to ethanol-mock treatment) or with the following additions: 1) PE5, PE6, PE8, PE12 or PE21 alone (each being used at the final concentration of 0.1%, 0.3%, 0.5% or 1.0%, see below); or 2) a pairwise combination of 0.1%, 0.3%, 0.5% or 1.0% PE5 and PE6, PE8, PE12 or PE21 (each being used at the final concentration of 0.1%, 0.3%, 0.5% or 1.0%).

We found that the longevity-extending efficiencies of the following pairwise combinations of aging-delaying PEs are statistically significantly greater than that of a PE component of the pair which was used as the HSA if added alone at the concentration exhibiting the highest aging-delaying effect: 1) a pairwise combination of 0.3% PE5 and 0.3% PE6 as compared to 0.5% PE5 (which was used as the HSA for both the mean and maximum CLS) (Supplementary Figure 3); 2) a pairwise combination of 0.1% PE5 and 0.1% PE8 as compared to 0.5% PE5 (which was considered as the HSA for the mean CLS) or 0.3% PE8 (which was considered as the HSA for the maximum CLS) (Figure 5); 3) a pairwise combination of 0.1% PE5 and 0.1% PE12 as compared to 0.5% PE5 (which was used as the HSA for the mean CLS) or 0.1% PE12 (which was used as the HSA for the maximum CLS) (Supplementary Figure 4); and 4) a pairwise combination of 0.1% PE5 and 0.1% PE21 as compared to 0.1% PE21 (which was used as the HSA for both the mean and maximum CLS) (Figure 6).

These findings confirm our hypothesis that pairwise combinations of PE5 and PE6, PE5 and PE8, PE5 and PE12, and PE5 and PE21 synergistically extend longevity of chronologically aging yeast.

Mixtures of PE6 and PE8, PE6 and PE12, and PE6 and PE21 synergistically extend longevity of chronologically aging yeast

Because PE6, PE8, PE12 and PE21 are known to affect different nodes, edges and modules of the signaling network that controls the rate of yeast chronological aging (Supplementary Figure 1) [87], we hypothesized that mixtures of PE6 with PE8, PE12 or PE21 may have synergistic effects on the efficiency of aging delay. To test this hypothesis, we cultured WT cells in the synthetic

minimal medium initially containing 2% glucose, either without a PE (i.e. cells were subjected to ethanol-mock treatment) or with the following additions: 1) PE6, PE8, PE12 or PE21 alone (each being used at the final concentration of 0.1%, 0.3% or 1.0%, see below); or 2) a mixture of 0.1%, 0.3%, 0.5% or 1.0% PE6 with PE8, PE12 or PE21 (each being used at the final concentration of 0.1%, 0.3%, 0.5% or 1.0%).

We found that the longevity-extending efficiencies of the following mixtures of aging-delaying PEs are statistically significantly greater than that of a PE component of the mixture which was considered as the HSA if used alone at the concentration having the maximum aging-delaying effect: 1) a mixture of 0.3% PE6 and 0.3% PE8 as compared to 1.0% PE6 (which was considered as the HSA for the mean CLS) or 0.3% PE8 (which was considered as the HSA for the maximum CLS) (Supplementary Figure 5); 2) a mixture of 0.3% PE6 and 0.1% PE12 as compared to 1.0% PE6 (which was used as the HSA for the mean CLS) or 0.1% PE12 (which was used as the HSA for the maximum CLS) (Figure 7); and 3) a mixture of 0.1% PE6 and 0.1% PE21 as compared to 0.1% PE21 (which was considered as the HSA for both the mean and maximum CLS) (Supplementary Figure 6).

Thus, in support of our hypothesis, mixtures of PE6 with PE8, PE12 or PE21 delay yeast chronological aging in a synergistic fashion.

Pairwise combinations of PE8 with PE12 or PE21 synergistically slow down yeast chronological aging

As has been noted above, PE8, PE12 and PE21 modulate different nodes, edges and modules of the signaling network that defines the rate of yeast chronological aging (Supplementary Figure 1) [87]. We therefore put forward the hypothesis that pairwise combinations of PE8 and PE12, and PE8 and PE21 may synergistically prolong longevity of chronologically aging yeast. To test this hypothesis, WT cells were cultured in the synthetic minimal medium initially containing 2% glucose, either without a PE (i.e. cells were subjected to ethanol-mock treatment) or with the following additions: 1) PE8, PE12 or PE21 alone (each being used at the final concentration of 0.1% or 0.3%, see below); or 2) a pairwise combination of 0.1%, 0.3%, 0.5% or 1.0% PE8 and PE12 or PE21 (each being used at the final concentration of 0.1%, 0.3%, 0.5% or 1.0%).

We found that the longevity-extending efficiencies of the following pairwise combinations of aging-delaying PEs statistically significantly exceed that of a PE component of the pair which was considered as the HSA if added alone at the concentration displaying the highest aging-delaying effect: 1) a pairwise combination of 0.1% PE8 and 0.1% PE12 as compared to 0.1% PE12 (which was considered as the HSA for both the mean and

maximum CLS) (Figure 8); and 2) a pairwise combination of 0.1% PE8 and 0.1% PE21 as compared to 0.1% PE21 (which was used as the HSA for both the mean and maximum CLS) (Supplementary Figure 7).

Taking together, these findings confirm our hypothesis that pairwise combinations of PE8 with PE12 or PE21 synergistically prolong longevity of chronologically aging yeast.

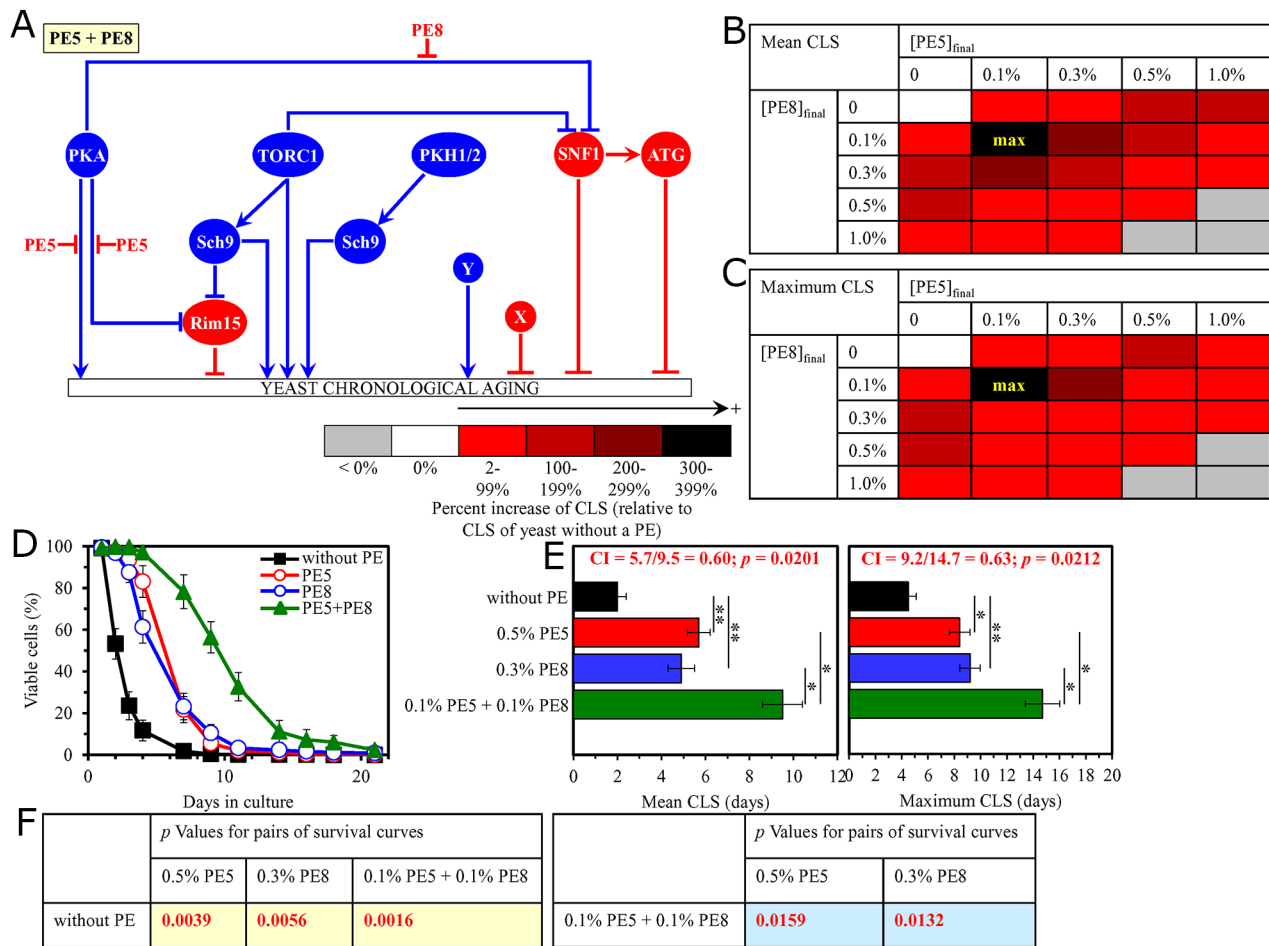


Figure 5: The longevity-extending efficiency of a mixture of 0.1% PE5 and 0.1% PE8 statistically significantly exceeds those of PE5 and PE8, which were used at the optimal concentration of 0.5% or 0.3% (respectively). Thus, PE5 and PE8 enhance the longevity-extending efficiency of each other. Hence, according to the HSA model, PE5 and PE8 act in synergy to extend longevity of chronologically aging yeast. **(A)** PE5 and PE8 are known to inhibit different pro-aging nodes of the signaling network that controls the rate of yeast chronological aging. PE5 mitigates two different branches of the pro-aging PKA pathway, whereas PE8 weakens the restraining action of this pathway on the anti-aging SNF1 pathway. **(B, C)** WT cells were grown as described in the legend to Figure 1, with PE5 and/or PE8 (at the final concentration of 0.1%, 0.3%, 0.5% or 1.0%) or without a PE. Effects of different concentrations of PE5 and PE8 (added alone or in pairwise combinations) on the mean (B) or maximum (C) CLS of WT cells are shown. The table cell at the intersection of the column for 0.1% PE5 and the row for 0.1% PE8 is marked "max" for the reason described in the legend to Figure 1. **(D, E)** WT cells were cultured as described in the legend to Figure 1, with one of the following supplements: 0.5% PE5, 0.3% PE8, or a mixture of 0.1% PE5 and 0.1% PE8. Ethanol was used as a vehicle or for mock treatment as described in the legend to Figure 1. Survival curves (D) and the mean and maximum lifespans (E) of chronologically aging WT cells cultured without a PE (cells were subjected to ethanol-mock treatment), with 0.5% PE5, with 0.3% PE8, or with the mixture of 0.1% PE5 and 0.1% PE8 are shown. Data in D and E are presented as means \pm SEM ($n = 3$; * $p < 0.05$; ** $p < 0.01$). The CI and p values in E were calculated as described in the legend to Figure 1. Data for mock-treated WT cells are replicated in graphs D and E of Figures 1–4, Figures 6–14 and Supplementary Figures 2–14. Data for WT cells cultured with 0.5% PE5 are replicated in graphs D and E of Figure 1, Figure 6, Figure 9, Supplementary Figure 3 and Supplementary Figure 4. Data for WT cells cultured with 0.3% PE8 are replicated in graphs D and E of Figure 2, Figure 8, Figure 10, Supplementary Figure 5, Supplementary Figure 7 and Supplementary Figure 14. **(F)** p Values for different pairs of survival curves of WT cells cultured in the presence of 0.5% PE5, 0.3% PE8, a mixture of 0.1% PE5 and 0.1% PE8, or in the absence of a PE (cells were subjected to ethanol-mock treatment) are shown. Survival curves shown in (D) were compared. The p values are displayed on a yellow or blue color background for the reasons described in the legend to Figure 1. Abbreviations: as in the legend to Figure 1.

A mixture of PE12 and PE21 slows down yeast chronological aging in a synergistic manner

Because PE12 and PE21 are known to affect two different nodes of the signaling network that controls the rate of yeast chronological aging (Supplementary

Figure 1) [87], we hypothesized that PE12 and PE21 may not act in synergy to delay yeast chronological aging. To test this hypothesis, we cultured WT cells in the synthetic minimal medium initially containing 2% glucose, either without a PE (i.e. cells were subjected to ethanol-mock treatment) or with the following

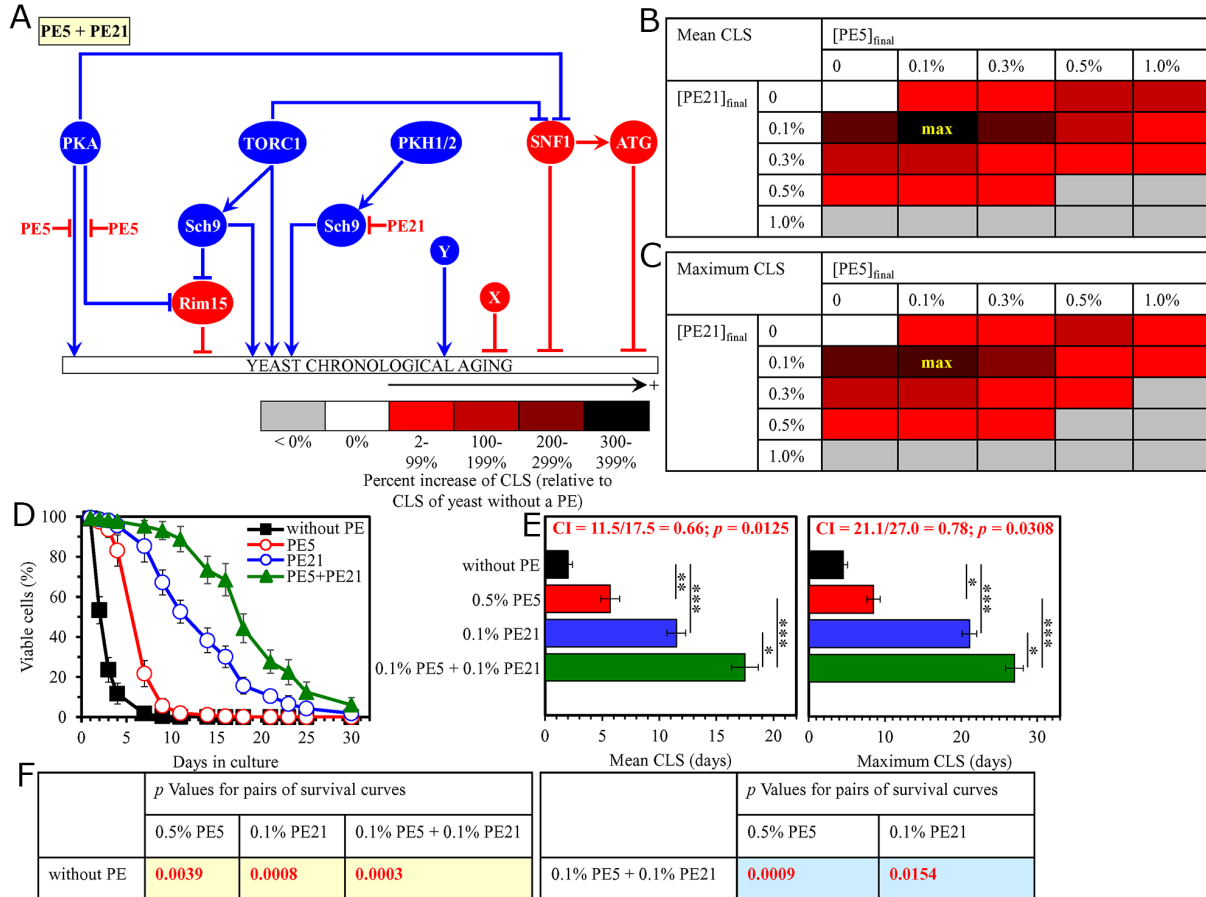


Figure 6: The longevity-extending efficiency of a mixture of 0.1% PE5 and 0.1% PE21 statistically significantly exceeds those of PE5 and PE21, which were used at the optimal concentration of 0.5% or 0.1% (respectively). Thus, PE5 and PE21 enhance the longevity-extending efficiency of each other. Hence, according to the HSA model, PE5 and PE21 act in synergy to extend longevity of chronologically aging yeast. **(A)** PE5 and PE21 are known to inhibit different pro-aging nodes of the signaling network that controls the rate of yeast chronological aging. PE5 mitigates two different branches of the pro-aging PKA pathway, whereas PE21 mitigates a form of the pro-aging protein kinase Sch9 that is activated by the pro-aging PKH1/2 pathway. **(B, C)** WT cells were grown as described in the legend to Figure 1, with PE5 and/or PE21 (at the final concentration of 0.1%, 0.3%, 0.5% or 1.0%) or without a PE. Effects of different concentrations of PE5 and PE21 (added alone or in pairwise combinations) on the mean (B) or maximum (C) CLS of WT cells are shown. The table cell at the intersection of the column for 0.1% PE5 and the row for 0.1% PE21 is marked "max" for the reason described in the legend to Figure 1. **(D, E)** WT cells were cultured as described in the legend to Figure 1, with one of the following supplements: 0.5% PE5, 0.1% PE21, or a mixture of 0.1% PE5 and 0.1% PE21. Ethanol was used as a vehicle or for mock treatment as described in the legend to Figure 1. Survival curves (D) and the mean and maximum lifespans (E) of chronologically aging WT cells cultured without a PE (cells were subjected to ethanol-mock treatment), with 0.5% PE5, with 0.1% PE21, or with the mixture of 0.1% PE5 and 0.1% PE21 are shown. Data in D and E are presented as means \pm SEM ($n = 3$; * $p < 0.05$; ** $p < 0.01$; *** $p < 0.001$). The CI and p values in E were calculated as described in the legend to Figure 1. Data for mock-treated WT cells are replicated in graphs D and E of Figures 1–5, Figures 7–14 and Supplementary Figures 2–14. Data for WT cells cultured with 0.5% PE5 are replicated in graphs D and E of Figure 1, Figure 5, Figure 9, Supplementary Figure 3 and Supplementary Figure 4. Data for WT cells cultured with 0.1% PE21 are replicated in graphs D and E of Figure 4, Figure 14, Supplementary Figures 6–8 and Supplementary Figure 12. **(F)** p Values for different pairs of survival curves of WT cells cultured in the presence of 0.5% PE5, 0.1% PE21, a mixture of 0.1% PE5 and 0.1% PE21, or in the absence of a PE (cells were subjected to ethanol-mock treatment) are shown. Survival curves shown in (D) were compared. The p values are displayed on a yellow or blue color background for the reasons described in the legend to Figure 1. Abbreviations: as in the legend to Figure 1.

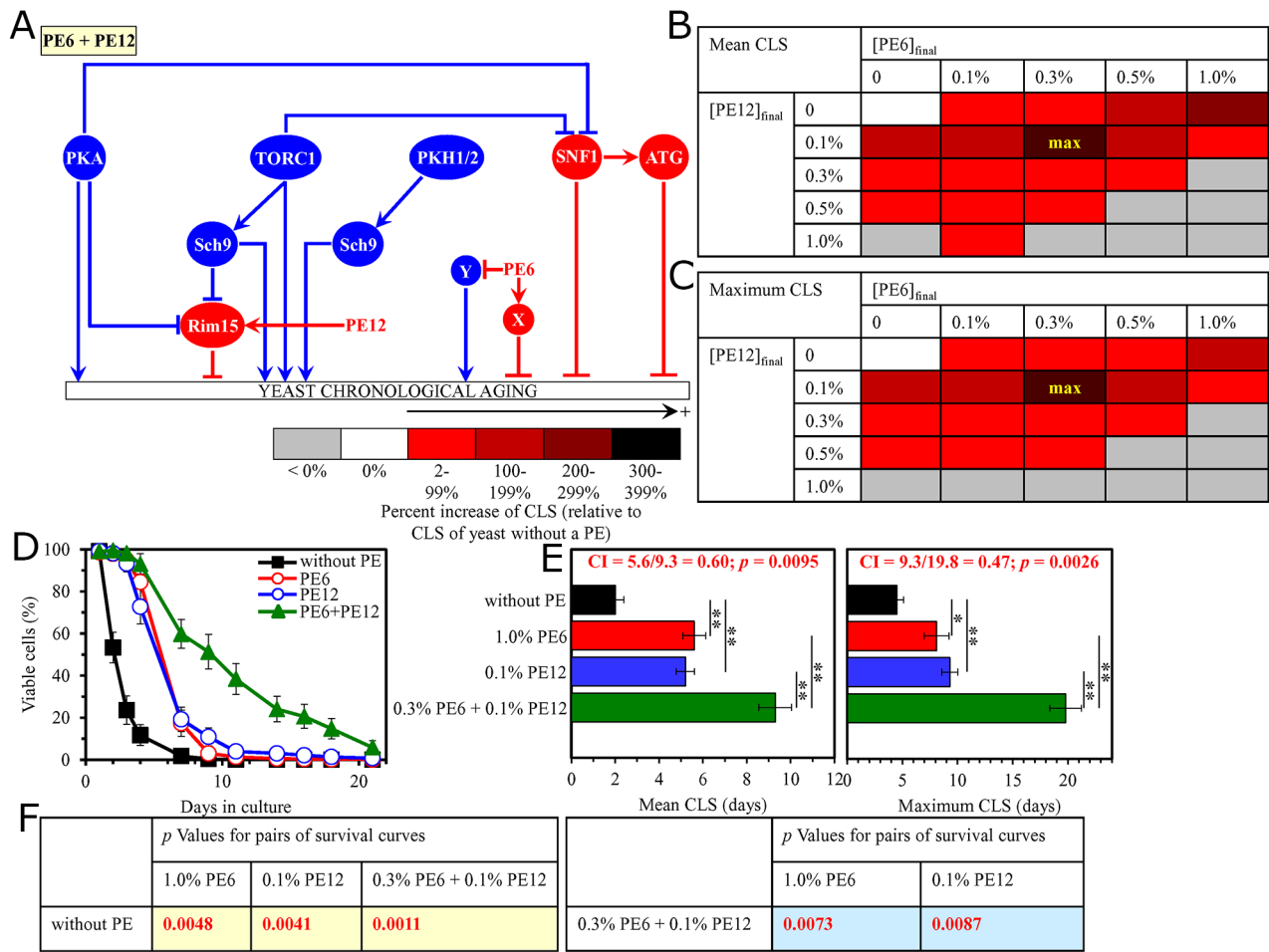


Figure 7: The longevity-extending efficiency of a mixture of 0.3% PE6 and 0.1% PE12 statistically significantly exceeds those of PE6 and PE12, which were used at the optimal concentration of 1.0% or 0.1% (respectively). Thus, PE6 and PE12 enhance the longevity-extending efficiency of each other. Hence, according to the HSA model, PE6 and PE12 act in synergy to extend longevity of chronologically aging yeast. (A) PE6 and PE12 are known to regulate different nodes of the signaling network that controls the rate of yeast chronological aging. PE12 stimulates the anti-aging protein kinase Rim15 assimilated into this signaling network, whereas PE6 modulates a presently unknown pro-aging or anti-aging node that may be integrated into this network. **(B, C)** WT cells were grown as described in the legend to Figure 1, with PE6 and/or PE12 (at the final concentration of 0.1%, 0.3%, 0.5% or 1.0%) or without a PE. Effects of different concentrations of PE6 and PE12 (added alone or in pairwise combinations) on the mean (B) or maximum (C) CLS of WT cells are shown. The table cell at the intersection of the column for 0.3% PE6 and the row for 0.1% PE12 is marked "max" for the reason described in the legend to Figure 1. **(D, E)** WT cells were cultured as described in the legend to Figure 1, with one of the following supplements: 1.0% PE6, 0.1% PE12, or a mixture of 0.3% PE6 and 0.1% PE12. Ethanol was used as a vehicle or for mock treatment as described in the legend to Figure 1. Survival curves (D) and the mean and maximum lifespans (E) of chronologically aging WT cells cultured without a PE (cells were subjected to ethanol-mock treatment), with 1.0% PE6, with 0.1% PE12, or with the mixture of 0.3% PE6 and 0.1% PE12 are shown. Data in D and E are presented as means \pm SEM ($n = 3$; * $p < 0.05$; ** $p < 0.01$). The CI and p values in E were calculated as described in the legend to Figure 1. Data for mock-treated WT cells are replicated in graphs D and E of Figures 1–6, Figures 8–14 and Supplementary Figures 2–14. Data for WT cells cultured with 1.0% PE6 are replicated in graphs D and E of Figure 12, Supplementary Figure 2, Supplementary Figure 3, Supplementary Figure 5, Supplementary Figure 6 and Supplementary Figure 10. Data for WT cells cultured with 0.1% PE12 are replicated in graphs D and E of Figure 3, Figure 8, Figure 13, Supplementary Figure 4, Supplementary Figure 8 and Supplementary Figure 11. **(F)** p Values for different pairs of survival curves of WT cells cultured in the presence of 1.0% PE6, 0.1% PE12, a mixture of 0.3% PE6 and 0.1% PE12, or in the absence of a PE (cells were subjected to ethanol-mock treatment) are shown. Survival curves shown in (D) were compared. The p values displayed on a yellow color background indicate that 1.0% PE6, 0.1% PE12, and the mixture of 0.3% PE6 and 0.1% PE12 significantly extend the CLS of WT cells. The p values are displayed on a yellow or blue color background for the reasons described in the legend to Figure 1. Abbreviations: as in the legend to Figure 1.

additions: 1) 0.1% PE12 or 0.1% PE21 alone (if PE12 or PE21 was used at this final concentration, it had the greatest longevity-extending effect); or 2) a mixture of 0.1%, 0.3%, 0.5% or 1.0% PE12 with 0.1%, 0.3%, 0.5% or 1.0% PE21).

In support of our hypothesis, we found that the longevity-extending efficiency of a mixture of 0.1% PE12 and 0.1% PE21 is statistically significantly greater than that of 0.1% PE21 (which was considered as the HSA if used alone at this concentration to attain the maximum aging-delaying effect) (Supplementary Figure 8).

Pairwise combinations of spermidine with PE4, PE5, PE6, PE8, PE12 or PE21 have synergistic effects on the extent of aging delay

Spermidine has been shown to delay yeast chronological aging by activating the anti-aging ATG1 pathway (Supplementary Figure 1) [88, 89, 92, 97, 100]. Neither PE4, PE5, PE6, PE8, PE12 nor PE21 affects the ATG1 node of the signaling network that defines the rate of yeast chronological aging (Supplementary Figure 1) [87]. We therefore hypothesized that pairwise combinations of spermidine with PE4, PE5, PE6, PE8, PE12 or PE21 may exhibit synergistic effects on the extent of yeast chronological aging delay. To test this hypothesis, WT cells were cultured in the synthetic minimal medium initially containing 2% glucose, either without a PE (i.e. cells were subjected to ethanol-mock treatment) or with the following additions: 1) PE4, PE5, PE6, PE8, PE12 or PE21 alone (each being used at the final concentration of 0.1%, 0.3%, 0.5% or 1.0%, see below); or 2) a mixture of 50 μM, 100 μM, 200 μM or 500 μM spermidine with PE4, PE5, PE6, PE8, PE12 or PE21 (each being used at the final concentration of 0.1%, 0.3%, 0.5% or 1.0%).

We found that the longevity-extending efficiencies of the following pairwise combinations of spermidine and an aging-delaying PE statistically significantly exceed that of a PE within the pair which was considered as the HSA (i.e. if this PE was used alone at the optimal aging-delaying concentration): 1) a mixture of 0.1% PE4 and 100 μM spermidine as compared to 0.5% PE4 (which was considered as the HSA for both the mean and maximum CLS) (Supplementary Figure 9); 2) a mixture of 0.3% PE5 and 100 μM spermidine as compared to 0.5% PE5 (which was used as the HSA for both the mean and maximum CLS) (Figure 9); 3) a mixture of 0.5% PE6 and 100 μM spermidine as compared to 1.0% PE6 (which was considered as the HSA for both the mean and maximum CLS) (Supplementary Figure 10); 4) a mixture of 0.1% PE8 and 100 μM spermidine as compared to 0.3% PE8 (which was used as the HSA for both the mean and maximum CLS) (Figure 10); 5) a mixture of 0.1% PE12 and 100 μM spermidine as compared to 0.1%

PE12 (which was considered as the HSA for both the mean and maximum CLS) (Supplementary Figure 11); and 6) a mixture of 0.1% PE21 and 100 μM spermidine as compared to 0.1% PE21 (which was used as the HSA for both the mean and maximum CLS) (Supplementary Figure 12).

These findings confirm our hypothesis that pairwise combinations of spermidine with PE4, PE5, PE6, PE8, PE12 or PE21 have synergistic effects on the extent of yeast chronological aging delay.

Mixtures of resveratrol with PE4, PE5, PE6, PE8, PE12 or PE21 synergistically slow down yeast chronological aging

Resveratrol modulates a presently unknown pro-aging or anti-aging node that may be integrated into the signaling network that controls the rate of yeast chronological aging (Supplementary Figure 1). PE4, PE5, PE8, PE12 and PE21 affect known nodes, edges and modules of this network, whereas PE6 (akin to resveratrol) regulates a currently unidentified node of the network (Supplementary Figure 1) [87]. Based on these observations, we put forward the following hypotheses: 1) mixtures of resveratrol with PE4, PE5, PE8, PE12 or PE21 may have synergistic effects on the efficiency of yeast chronological aging delay; 2) if resveratrol and PE6 target different nodes of the network, their mixture may delay yeast chronological aging in a synergistic manner; and 3) if resveratrol and PE6 target the same node of the network, resveratrol and PE6 may not act in synergy to slow down yeast chronological aging. To test these hypotheses, we cultured WT cells in the synthetic minimal medium initially containing 2% glucose, either without a PE (i.e. cells were subjected to ethanol-mock treatment) or with the following additions: 1) PE4, PE5, PE6, PE8, PE12 or PE21 alone (each being used at the final concentration of 0.1%, 0.3%, 0.5% or 1.0%, see below); or 2) a mixture of 10 μM, 20 μM, 50 μM or 100 μM resveratrol with PE4, PE5, PE6, PE8, PE12 or PE21 (each being used at the final concentration of 0.1%, 0.3%, 0.5% or 1.0%).

We found that the longevity-extending efficiencies of the following mixtures of resveratrol and an aging-delaying PE are statistically significantly greater than that of a PE within the mixture which was used as the HSA (i.e. if this PE was added alone at the optimal aging-delaying concentration): 1) a mixture of 0.5% PE4 and 50 μM resveratrol as compared to 0.5% PE4 (which was used as the HSA for both the mean and maximum CLS) (Figure 11); 2) a mixture of 0.3% PE5 and 50 μM resveratrol as compared to 0.5% PE5 (which was considered as the HSA for both the mean and maximum CLS) (Supplementary Figure 13); 3) a mixture of 0.5% PE6 and 50 μM resveratrol as compared to 1.0% PE6 (which was used as the HSA for both the mean and

maximum CLS) (Figure 12); 4) a mixture of 0.3% PE8 and 50 μM resveratrol as compared to 0.3% PE8 (which was considered as the HSA for both the mean and maximum CLS) (Supplementary Figure 14); 5) a mixture of 0.1% PE12 and 50 μM resveratrol as compared to 0.1% PE12 (which was used as the HSA for both the

mean and maximum CLS) (Figure 13); and 6) a mixture of 0.1% PE21 and 50 μM resveratrol as compared to 0.1% PE21 (which was considered as the HSA for both the mean and maximum CLS) (Figure 14).

In sum, these findings confirm the following hypotheses: 1) mixtures of resveratrol with PE4, PE5, PE8,

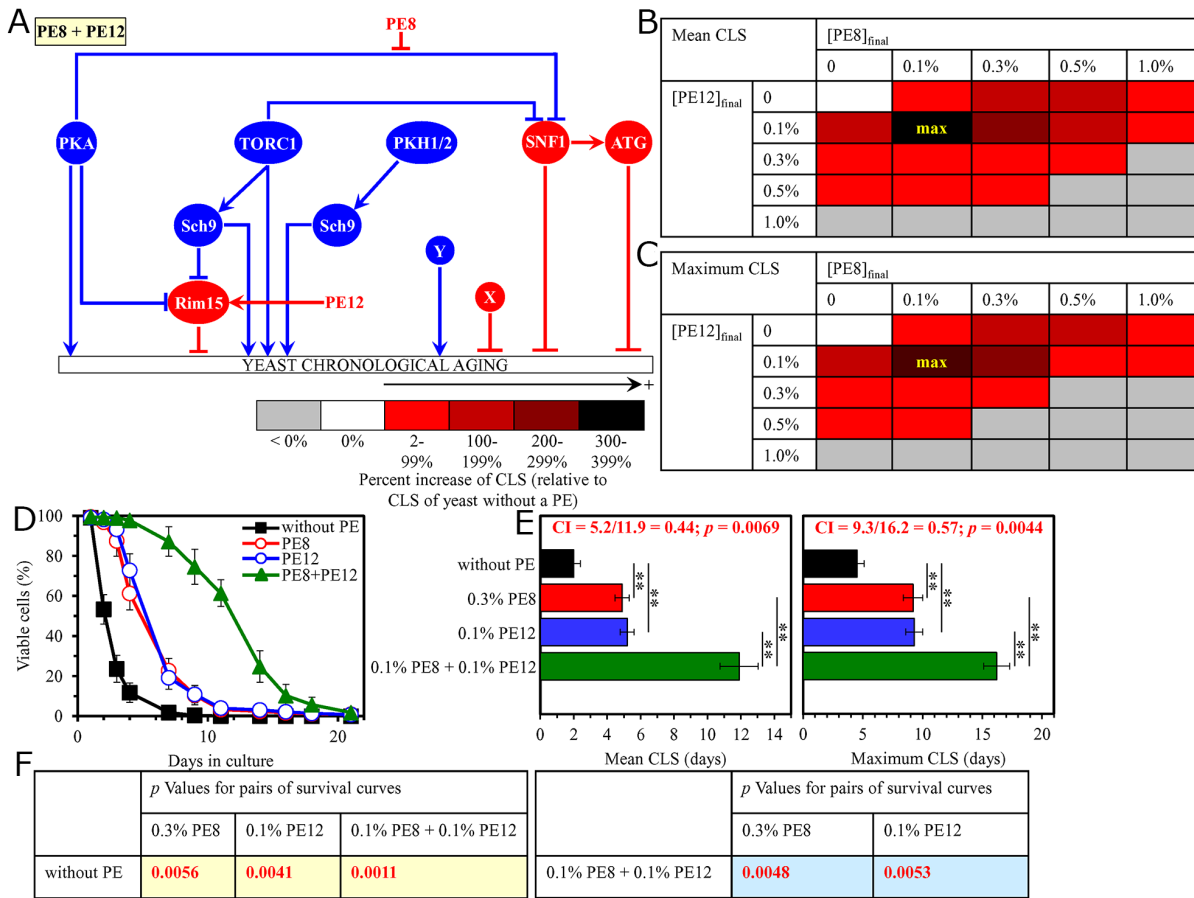


Figure 8: The longevity-extending efficiency of a mixture of 0.1% PE8 and 0.1% PE12 statistically significantly exceeds those of PE8 and PE12, which were used at the optimal concentration of 0.3% or 0.1% (respectively). Thus, PE8 and PE12 enhance the longevity-extending efficiency of each other. Hence, according to the HSA model, PE8 and PE12 act in synergy to extend longevity of chronologically aging yeast. **(A)** PE8 and PE12 are known to regulate different nodes of the signaling network that controls the rate of yeast chronological aging. PE8 weakens the restraining action of the pro-aging PKA pathway on the anti-aging SNF1 pathway, whereas PE12 stimulates the anti-aging protein kinase Rim15 integrated into this signaling network. **(B, C)** WT cells were grown as described in the legend to Figure 1, with PE8 and/or PE12 (at the final concentration of 0.1%, 0.3%, 0.5% or 1.0%) or without a PE. Effects of different concentrations of PE8 and PE12 (added alone or in pairwise combinations) on the mean (B) or maximum (C) CLS of WT cells are shown. The table cell at the intersection of the column for 0.1% PE8 and the row for 0.1% PE12 is marked "max" for the reason described in the legend to Figure 1. **(D, E)** WT cells were cultured as described in the legend to Figure 1, with one of the following supplements: 0.3% PE8, 0.1% PE12, or a mixture of 0.1% PE8 and 0.1% PE12. Ethanol was used as a vehicle or for mock treatment as described in the legend to Figure 1. Survival curves (D) and the mean and maximum lifespans (E) of chronologically aging WT cells cultured without a PE (cells were subjected to ethanol-mock treatment), with 0.3% PE8, with 0.1% PE12, or with the mixture of 0.1% PE8 and 0.1% PE12 are shown. Data in D and E are presented as means ± SEM ($n = 3$; ** $p < 0.01$). The CI and p values in E were calculated as described in the legend to Figure 1. Data for mock-treated WT cells are replicated in graphs D and E of Figures 1–7, Figures 9–14 and Supplementary Figures 2–14. Data for WT cells cultured with 0.3% PE8 are replicated in graphs D and E of Figure 2, Figure 5, Figure 10, Supplementary Figure 5, Supplementary Figure 7 and Supplementary Figure 14. Data for WT cells cultured with 0.1% PE12 are replicated in graphs D and E of Figure 3, Figure 7, Figure 13, Supplementary Figure 4, Supplementary Figure 8 and Supplementary Figure 11. **(F)** p Values for different pairs of survival curves of WT cells cultured in the presence of 0.3% PE8, 0.1% PE12, a mixture of 0.1% PE8 and 0.1% PE12, or in the absence of a PE (cells were subjected to ethanol-mock treatment) are shown. Survival curves shown in (D) were compared. The p values are displayed on a yellow or blue color background for the reasons described in the legend to Figure 1. Abbreviations: as in the legend to Figure 1.

PE12 or PE21 exhibit synergistic effects on the efficiency of yeast chronological aging delay; and 2) if resveratrol and PE6 target different nodes of the network, a mixture of resveratrol and PE6 delays yeast chronological aging in a synergistic manner.

DISCUSSION

The objective of this proof-of-concept study was to test our hypothesis that a mixture of two aging-delaying

PEs or a combination of one of these PEs and spermidine or resveratrol may delay yeast chronological aging and extend yeast longevity in a synergistic fashion only if each of the two components of this mixture affects a different node, edge or module of the signaling network of longevity regulation. To attain this objective, we performed a systematic assessment of longevity-extending proficiencies of all possible pairwise combinations of PE4, PE5, PE6, PE8, PE12 and PE21 or of one of these PEs and spermidine or resveratrol in chronologically aging *S. cerevisiae*. In

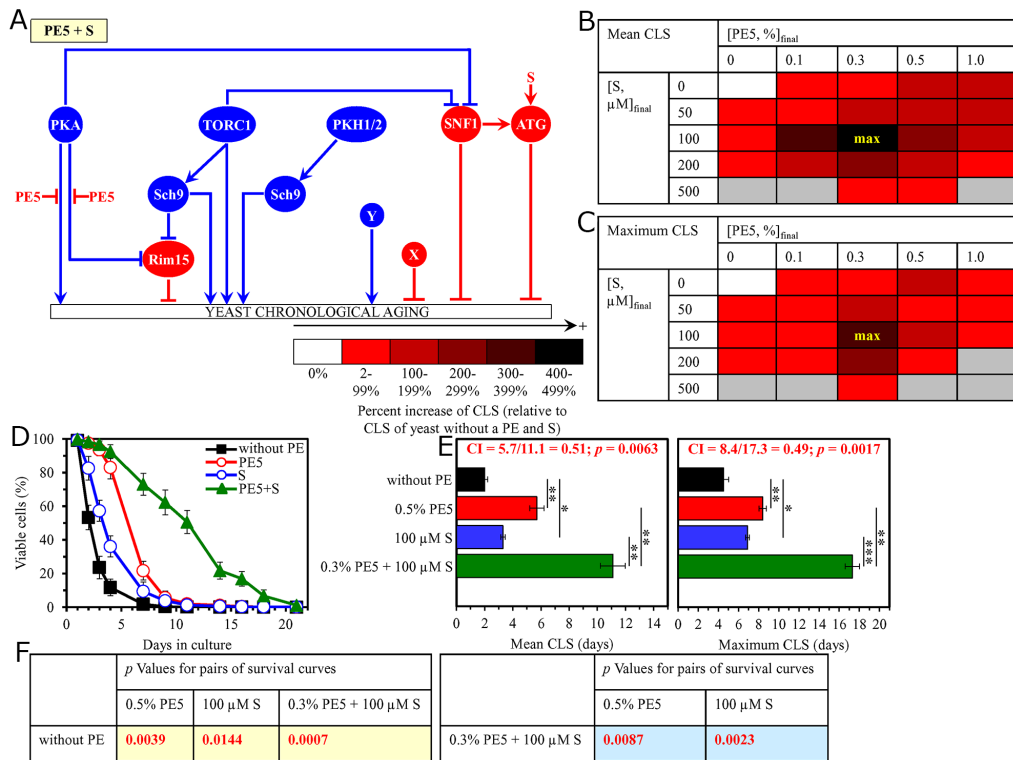


Figure 9: The longevity-extending efficiency of a mixture of 0.3% PE5 and 100 μM spermidine (S) statistically significantly exceeds those of PE5 and S, which were used at the optimal concentration of 0.5% or 100 μM (respectively). Thus, PE5 and S enhance the longevity-extending efficiency of each other. Hence, according to the HSA model, PE5 and S act in synergy to extend longevity of chronologically aging yeast. **(A)** PE5 and S are known to regulate different nodes of the signaling network that controls the rate of yeast chronological aging. PE5 mitigates two different branches of the pro-aging PKA pathway, whereas S stimulates the anti-aging ATG pathway. **(B, C)** WT cells were grown as described in the legend to Figure 1, with PE5 (at the final concentration of 0.1%, 0.3%, 0.5% or 1.0%) and/or S (at the final concentration of 50 μM, 100 μM, 200 μM or 500 μM), or without a PE and S. Effects of different concentrations of PE5 and S (added alone or in pairwise combinations) on the mean (B) or maximum (C) CLS of WT cells are shown. The table cell at the intersection of the column for 0.3% PE5 and the row for 100 μM S is marked "max" for the reason described in the legend to Figure 1. **(D, E)** WT cells were cultured as described in the legend to Figure 1, with one of the following supplements: 0.5% PE5, 100 μM S, or a mixture of 0.3% PE5 and 100 μM S. Ethanol was used as a vehicle or for mock treatment as described in the legend to Figure 1. Survival curves (D) and the mean and maximum lifespans (E) of chronologically aging WT cells cultured without a PE and S (cells were subjected to ethanol-mock treatment), with 0.5% PE5, with 100 μM S, or with the mixture of 0.3% PE5 and 100 μM S are shown. Data in D and E are presented as means ± SEM ($n = 3$; * $p < 0.05$; ** $p < 0.01$; *** $p < 0.001$). The CI and p values in E were calculated as described in the legend to Figure 1. Data for mock-treated WT cells are replicated in graphs D and E of Figures 1–8, Figures 10–14 and Supplementary Figures 2–14. Data for WT cells cultured with 0.5% PE5 are replicated in graphs D and E of Figure 1, Figure 5, Figure 6, Supplementary Figure 3 and Supplementary Figure 4. Data for WT cells cultured with 100 μM S are replicated in graphs D and E of Figure 10 and Supplementary Figures 9–12. **(F)** p Values for different pairs of survival curves of WT cells cultured in the presence of 0.5% PE5, 100 μM S, a mixture of 0.3% PE5 and 100 μM S, or in the absence of a PE and S (cells were subjected to ethanol-mock treatment) are shown. Survival curves shown in (D) were compared. The p values are displayed on a yellow or blue color background for the reasons described in the legend to Figure 1. Abbreviations: as in the legend to Figure 1.

support of our hypothesis, we provided evidence that pairwise combinations of naturally-occurring chemical compounds that slow yeast chronological aging through different nodes, edges and modules of this evolutionarily conserved network exhibit synergistic effects on the magnitude of aging delay. It needs to be emphasized that studies in mice, fruit flies, aquatic invertebrates, nematodes, and budding and fission yeast have recently demonstrated

that a two- or three-component combination of the aging-delaying chemical compounds that target different aging-associated processes or signaling pathways synergistically delay aging and prolong healthy lifespan [79–85]. Given that the major aspects and basic mechanisms of aging and aging-associated pathology have been conserved over the course of evolution [64, 67, 88, 91, 94–102], findings in budding yeast presented here and the above findings in

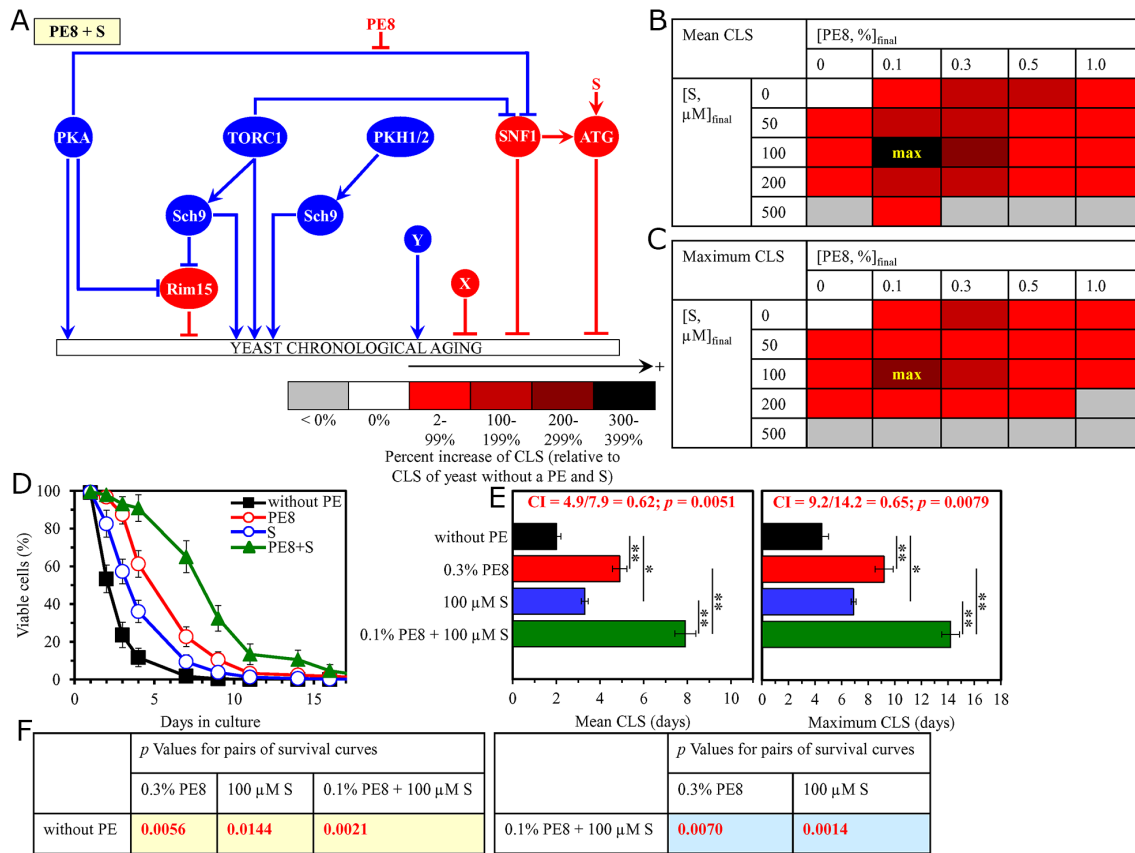


Figure 10: The longevity-extending efficiency of a mixture of 0.1% PE8 and 100 μM spermidine (S) statistically significantly exceeds those of PE8 and S, which were used at the optimal concentration of 0.3% or 100 μM (respectively). Thus, PE8 and S enhance the longevity-extending efficiency of each other. Hence, according to the HSA model, PE8 and S act in synergy to extend longevity of chronologically aging yeast. **(A)** PE8 and S are known to regulate different nodes of the signaling network that controls the rate of yeast chronological aging. PE8 weakens the restraining action of the pro-aging PKA pathway on the anti-aging SNF1 pathway, whereas S stimulates the anti-aging ATG pathway. **(B, C)** WT cells were grown as described in the legend to Figure 1, with PE8 (at the final concentration of 0.1%, 0.3%, 0.5% or 1.0%) and/or S (at the final concentration of 50 μM, 100 μM, 200 μM or 500 μM), or without a PE and S. Effects of different concentrations of PE8 and S (added alone or in pairwise combinations) on the mean (B) or maximum (C) CLS of WT cells are shown. The table cell at the intersection of the column for 0.1% PE8 and the row for 100 μM S is marked "max" for the reason described in the legend to Figure 1. **(D, E)** WT cells were cultured as described in the legend to Figure 1, with one of the following supplements: 0.3% PE8, 100 μM S, or a mixture of 0.1% PE8 and 100 μM S. Ethanol was used as a vehicle or for mock treatment as described in the legend to Figure 1. Survival curves (D) and the mean and maximum lifespans (E) of chronologically aging WT cells cultured without a PE and S (cells were subjected to ethanol-mock treatment), with 0.3% PE8, with 100 μM S, or with the mixture of 0.1% PE8 and 100 μM S are shown. Data in D and E are presented as means ± SEM ($n = 3$; * $p < 0.05$; ** $p < 0.01$). The CI and p values in E were calculated as described in the legend to Figure 1. Data for mock-treated WT cells are replicated in graphs D and E of Figures 1–9, Figures 11–14 and Supplementary Figures 2–14. Data for WT cells cultured with 0.3% PE8 are replicated in graphs D and E of Figure 2, Figure 5, Figure 8, Supplementary Figure 5, Supplementary Figure 7 and Supplementary Figure 14. Data for WT cells cultured with 100 μM S are replicated in graphs D and E of Figure 9 and Supplementary Figures 9–12. **(F)** p Values for different pairs of survival curves of WT cells cultured in the presence of 0.3% PE8, 100 μM S, a mixture of 0.1% PE8 and 100 μM S, or in the absence of a PE and S (cells were subjected to ethanol-mock treatment) are shown. Survival curves shown in (D) were compared. The p values are displayed on a yellow or blue color background for the reasons described in the legend to Figure 1. Abbreviations: as in the legend to Figure 1.

other model eukaryotic organisms [79–85] support the proposed idea [74–78] that multicomponent combinations of chemical compounds that target different aging-associated processes or signaling pathways can be used for therapeutic multiplexing of aging delay and healthspan improvement in humans.

Of note, our recent study has revealed that PE4, PE5, PE6, PE8, PE12 and PE21 are geroprotectors that delay the onset and decrease the rate of yeast chronological aging by triggering a hormetic stress response and differently altering the following longevity-defining cellular processes: 1) the maintenance of mitochondrial respiration

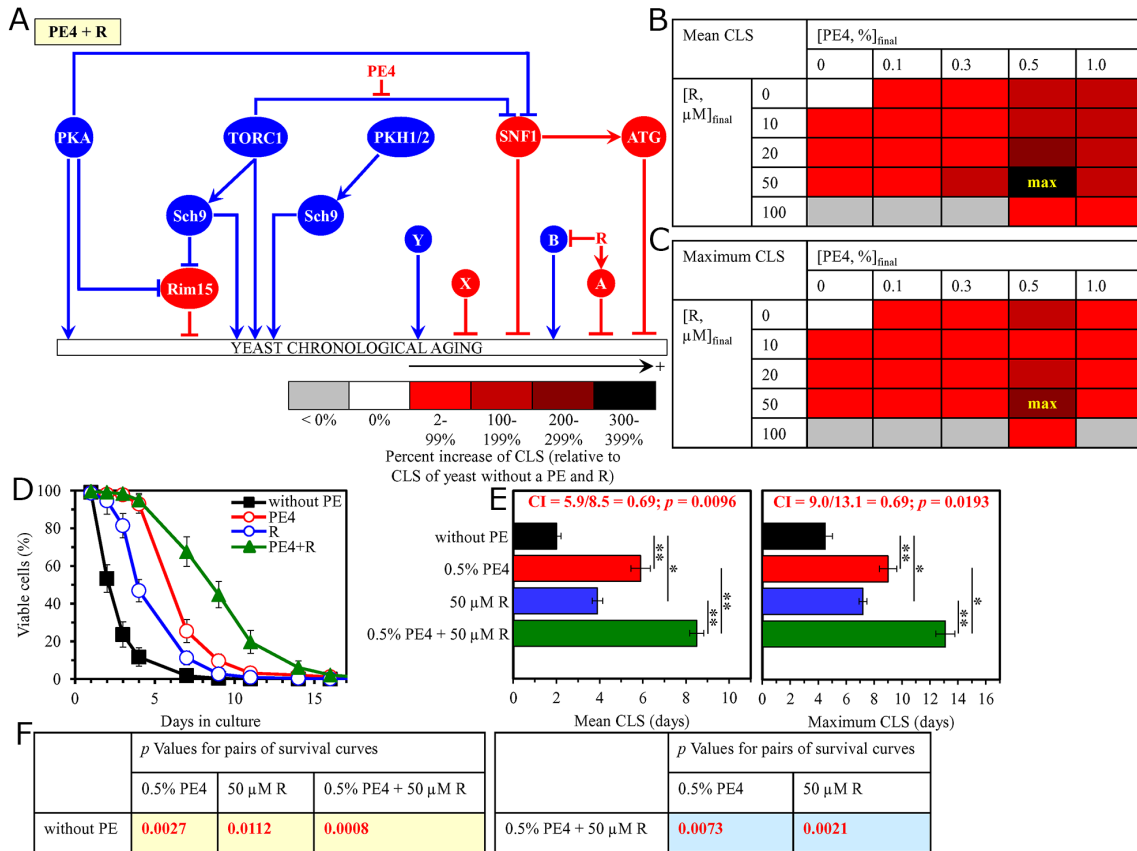


Figure 11: The longevity-extending efficiency of a mixture of 0.5% PE4 and 50 μM resveratrol (R) statistically significantly exceeds those of PE4 and R, which were used at the optimal concentration of 0.5% or 50 μM (respectively). Thus, PE4 and R enhance the longevity-extending efficiency of each other. Hence, according to the HSA model, PE4 and R act in synergy to extend longevity of chronologically aging yeast. **(A)** PE4 and R are known to regulate different nodes of the signaling network that controls the rate of yeast chronological aging. PE4 weakens the restraining action of the pro-aging TORC1 pathway on the anti-aging SNF1 pathway, whereas R modulates a presently unknown pro-aging or anti-aging node that may be integrated into this signaling network. **(B, C)** WT cells were grown as described in the legend to Figure 1, with PE4 (at the final concentration of 0.1%, 0.3%, 0.5% or 1.0%) and/or R (at the final concentration of 10 μM , 20 μM , 50 μM or 100 μM), or without a PE and R. Effects of different concentrations of PE4 and R (added alone or in pairwise combinations) on the mean (B) or maximum (C) CLS of WT cells are shown. The table cell at the intersection of the column for 0.5% PE4 and the row for 50 μM R is marked "max" for the reason described in the legend to Figure 1. **(D, E)** WT cells were cultured as described in the legend to Figure 1, with one of the following supplements: 0.5% PE4, 50 μM R, or a mixture of 0.5% PE4 and 50 μM R. Ethanol was used as a vehicle or for mock treatment as described in the legend to Figure 1. Survival curves (D) and the mean and maximum lifespans (E) of chronologically aging WT cells cultured without a PE and R (cells were subjected to ethanol-mock treatment), with 0.5% PE4, with 50 μM R, or with the mixture of 0.5% PE4 and 50 μM R are shown. Data in D and E are presented as means \pm SEM ($n = 3$; * $p < 0.05$; ** $p < 0.01$). The CI and p values in E were calculated as described in the legend to Figure 1. Data for mock-treated WT cells are replicated in graphs D and E of Figures 1–10, Figure 2, Figures 12–14 and Supplementary Figures 2–14. Data for WT cells cultured with 0.5% PE4 are replicated in graphs D and E of Figures 1–4, Figure 11, Supplementary Figure 2 and Supplementary Figure 9. Data for WT cells cultured with 50 μM R are replicated in graphs D and E of Figures 12–14, Supplementary Figure 13 and Supplementary Figure 14. **(F)** p Values for different pairs of survival curves of WT cells cultured in the presence of 0.5% PE4, 50 μM R, a mixture of 0.5% PE4 and 50 μM R, or in the absence of a PE and R (cells were subjected to ethanol-mock treatment) are shown. Survival curves shown in (D) were compared. The p values are displayed on a yellow or blue color background for the reasons described in the legend to Figure 1. Abbreviations: A, a presently unknown anti-aging node of the signaling network; B, a presently unknown pro-aging node of the signaling network; other abbreviations are as in the legend to Figure 1.

and membrane potential; 2) the preservation of reactive oxygen species homeostasis; 3) the protection of cellular proteins, membrane lipids, and mitochondrial and nuclear genomes from oxidative damage; 4) cell defense from

acute oxidative and thermal stresses; and 5) the lipolytic degradation of neutral lipids deposited in lipid droplets [86]. In the future, it would be interesting to investigate how the two-component mixes of the six aging-delaying

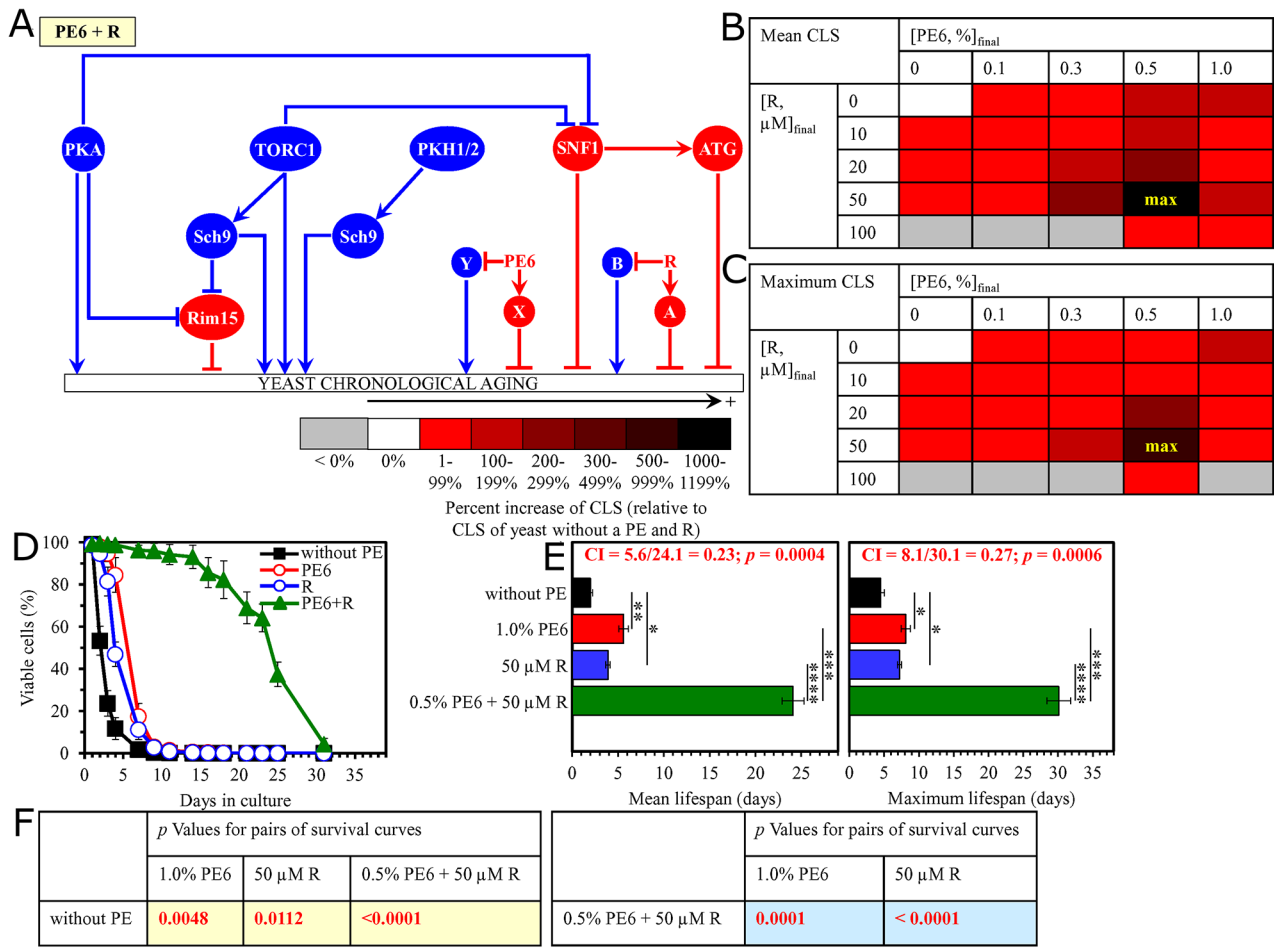


Figure 12: The longevity-extending efficiency of a mixture of 0.5% PE6 and 50 μM resveratrol (R) statistically significantly exceeds those of PE6 and R, which were used at the optimal concentration of 1.0% or 50 μM (respectively). Thus, PE6 and R enhance the longevity-extending efficiency of each other. Hence, according to the HSA model, PE6 and R act in synergy to extend longevity of chronologically aging yeast. **(A)** PE6 and R regulate different pro-aging or anti-aging nodes that may be integrated into the signaling network controlling the rate of yeast chronological aging; the identities of proteins that form these nodes are presently unknown. **(B, C)** WT cells were grown as described in the legend to Figure 1, with PE6 (at the final concentration of 0.1%, 0.3%, 0.5% or 1.0%) and/or R (at the final concentration of 10 μM, 20 μM, 50 μM or 100 μM), or without a PE and R. Effects of different concentrations of PE6 and R (added alone or in pairwise combinations) on the mean (B) or maximum (C) CLS of WT cells are shown. The table cell at the intersection of the column for 0.5% PE6 and the row for 50 μM R is marked "max" for the reason described in the legend to Figure 1. **(D, E)** WT cells were cultured as described in the legend to Figure 1, with one of the following supplements: 0.5% PE6, 50 μM R, or a mixture of 0.5% PE6 and 50 μM R. Ethanol was used as a vehicle or for mock treatment as described in the legend to Figure 1. Survival curves (D) and the mean and maximum lifespans (E) of chronologically aging WT cells cultured without a PE and R (cells were subjected to ethanol-mock treatment), with 1.0% PE6, with 50 μM R, or with the mixture of 0.5% PE6 and 50 μM R are shown. Data in D and E are presented as means ± SEM ($n = 3$; * $p < 0.05$; ** $p < 0.01$; *** $p < 0.001$; **** $p < 0.0001$). The CI and p values in E were calculated as described in the legend to Figure 1. Data for mock-treated WT cells are replicated in graphs D and E of Figures 1–11, Figure 13, Figure 14 and Supplementary Figures 2–14. Data for WT cells cultured with 1.0% PE6 are replicated in graphs D and E of Figure 7, Supplementary Figure 2, Supplementary Figure 3, Supplementary Figure 5, Supplementary Figure 6 and Supplementary Figure 10. Data for WT cells cultured with 50 μM R are replicated in graphs D and E of Figure 11, Figure 13, Figure 14, Supplementary Figure 13 and Supplementary Figure 14. **(F)** p Values for different pairs of survival curves of WT cells cultured in the presence of 1.0% PE6, 50 μM R, a mixture of 0.5% PE6 and 50 μM R, or in the absence of a PE and R (cells were subjected to ethanol-mock treatment) are shown. Survival curves shown in (D) were compared. The p values are displayed on a yellow or blue color background for the reasons described in the legend to Figure 1. Abbreviations: as in the legend to Figure 1.

PEs that synergistically delay yeast chronological aging influence each of these cellular processes. This will allow us to gain insight into the mechanisms through which

each of these pairwise combinations of PEs can delay the onset and decelerate the progression of the cellular aging process.

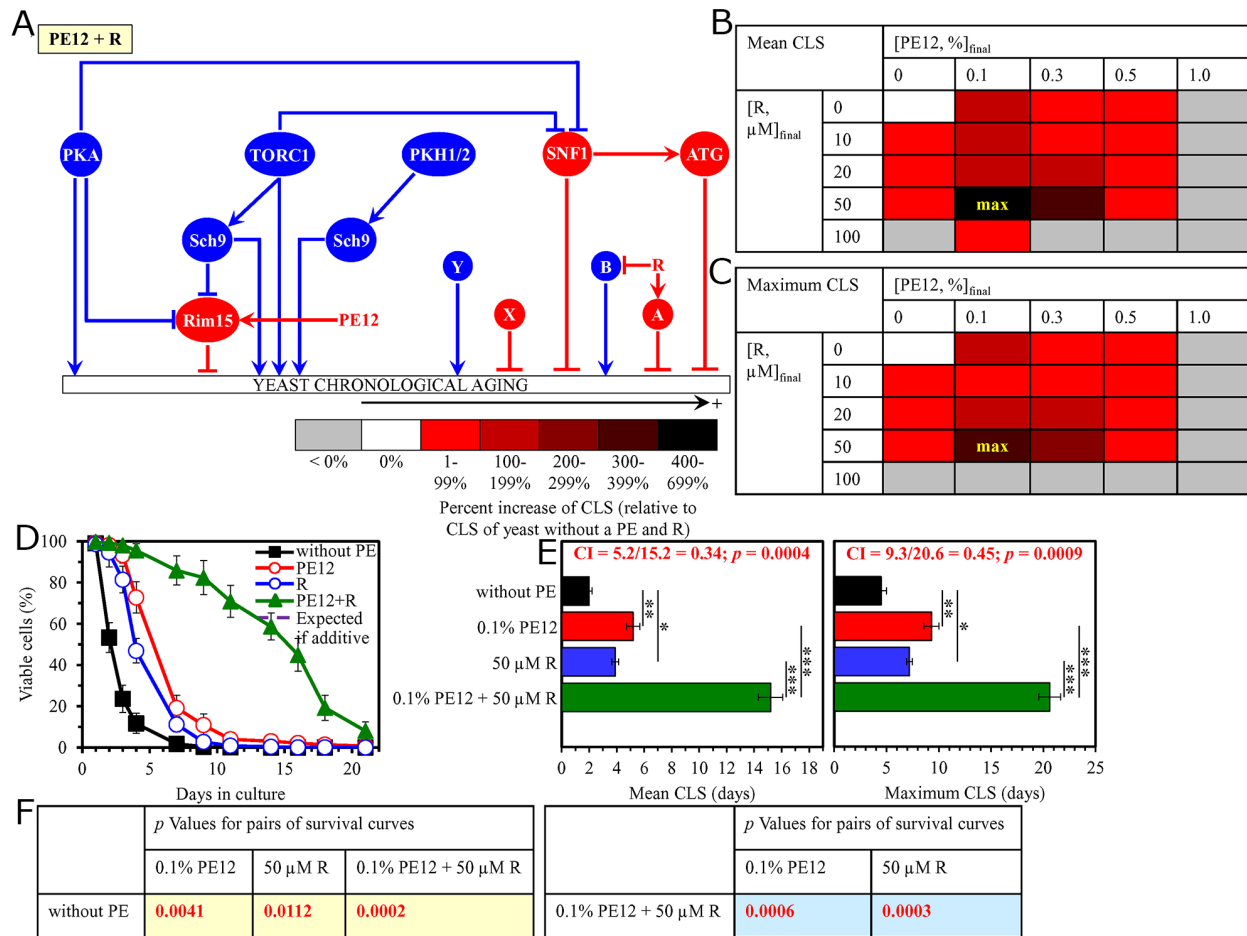


Figure 13: The longevity-extending efficiency of a mixture of 0.1% PE12 and 50 μM resveratrol (R) statistically significantly exceeds those of PE12 and R, which were used at the optimal concentration of 0.1% or 50 μM (respectively). Thus, PE12 and R enhance the longevity-extending efficiency of each other. Hence, according to the HSA model, PE12 and R act in synergy to extend longevity of chronologically aging yeast. **(A)** PE12 and R regulate different nodes of the signaling network that controls the rate of yeast chronological aging. PE12 stimulates the anti-aging protein kinase Rim15, whereas R modulates a presently unknown pro-aging or anti-aging node that may be integrated into this signaling network. **(B, C)** WT cells were grown as described in the legend to Figure 1, with PE12 (at the final concentration of 0.1%, 0.3%, 0.5% or 1.0%) and/or R (at the final concentration of 10 μM , 20 μM , 50 μM or 100 μM), or without a PE and R. Effects of different concentrations of PE12 and R (added alone or in pairwise combinations) on the mean (B) or maximum (C) CLS of WT cells are shown. The table cell at the intersection of the column for 0.1% PE12 and the row for 50 μM R is marked "max" for the reason described in the legend to Figure 1. **(D, E)** WT cells were cultured as described in the legend to Figure 1, with one of the following supplements: 0.1% PE12, 50 μM R, or a mixture of 0.1% PE12 and 50 μM R. Ethanol was used as a vehicle or for mock treatment as described in the legend to Figure 1. Survival curves (D) and the mean and maximum lifespans (E) of chronologically aging WT cells cultured without a PE and R (cells were subjected to ethanol-mock treatment), with 0.1% PE12, with 50 μM R, or with the mixture of 0.1% PE12 and 50 μM R are shown. Data in D and E are presented as means \pm SEM ($n = 3$; * $p < 0.05$; ** $p < 0.01$; *** $p < 0.001$). The CI and p values in E were calculated as described in the legend to Figure 1. Data for mock-treated WT cells are replicated in graphs D and E of Figures 1–12, Figure 14 and Supplementary Figures 2–14. Data for WT cells cultured with 0.1% PE12 are replicated in graphs D and E of Figure 3, Figure 7, Figure 8, Supplementary Figure 4, Supplementary Figure 8 and Supplementary Figure 11. Data for WT cells cultured with 50 μM R are replicated in graphs D and E of Figure 11, Figure 12, Figure 14, Supplementary Figure 13 and Supplementary Figure 14. **(F)** p Values for different pairs of survival curves of WT cells cultured in the presence of 0.1% PE12, 50 μM R, a mixture of 0.1% PE12 and 50 μM R, or in the absence of a PE and R (cells were subjected to ethanol-mock treatment) are shown. Survival curves shown in (D) were compared. The p values are displayed on a yellow or blue color background for the reasons described in the legend to Figure 1. Abbreviations: as in the legend to Figure 1.

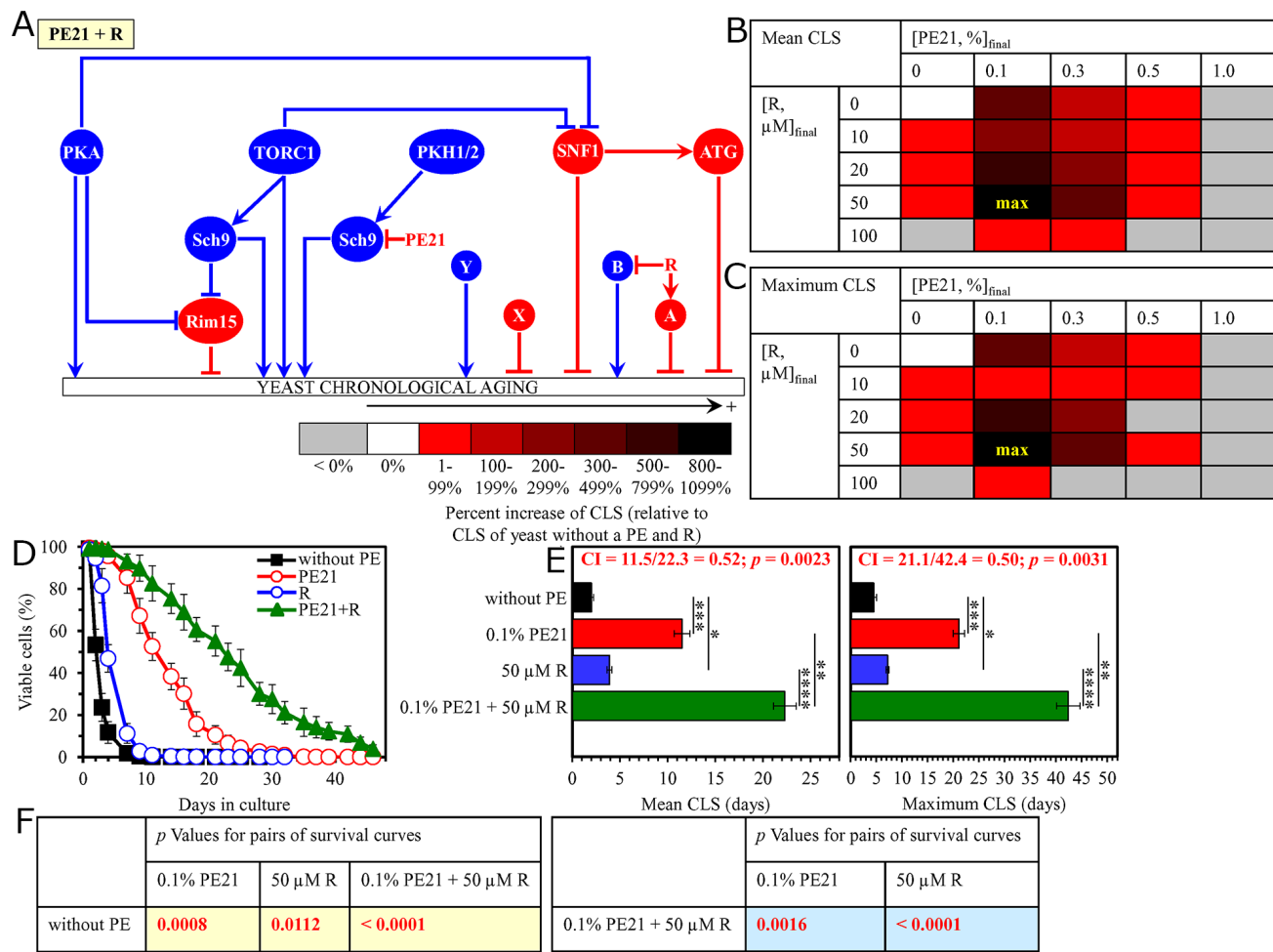


Figure 14: The longevity-extending efficiency of a mixture of 0.1% PE21 and 50 μM resveratrol (R) statistically significantly exceeds those of PE21 and R, which were used at the optimal concentration of 0.1% or 50 μM (respectively). Thus, PE21 and R enhance the longevity-extending efficiency of each other. Hence, according to the HSA model, PE21 and R act in synergy to extend longevity of chronologically aging yeast. (A) PE21 and R regulate different nodes of the signaling network that controls the rate of yeast chronological aging. PE21 mitigates a form of the pro-aging protein kinase Sch9 that is activated by the pro-aging PKH1/2 pathway, whereas R modulates a presently unknown pro-aging or anti-aging node that may be integrated into this signaling network. (B, C) WT cells were grown as described in the legend to Figure 1, with PE21 (at the final concentration of 0.1%, 0.3%, 0.5% or 1.0%) and/or R (at the final concentration of 10 μM , 20 μM , 50 μM or 100 μM), or without a PE and R. Effects of different concentrations of PE21 and R (added alone or in pairwise combinations) on the mean (B) or maximum (C) CLS of WT cells are shown. The table cell at the intersection of the column for 0.1% PE21 and the row for 50 μM R is marked "max" for the reason described in the legend to Figure 1. (D, E) WT cells were cultured in the synthetic minimal YNB medium initially containing 2% glucose and one of the following supplements: 0.1% PE21, 50 μM R, or a mixture of 0.1% PE21 and 50 μM R. Ethanol was used as a vehicle or for mock treatment as described in the legend to Figure 1. Survival curves (D) and the mean and maximum lifespans (E) of chronologically aging WT cells cultured without a PE and R (cells were subjected to ethanol-mock treatment), with 0.1% PE21, with 50 μM R, or with the mixture of 0.1% PE21 and 50 μM R are shown. Data in D and E are presented as means \pm SEM ($n = 3$; * $p < 0.05$; ** $p < 0.01$; *** $p < 0.001$; **** $p < 0.0001$). The CI and p values in E were calculated as described in the legend to Figure 1. Data for mock-treated WT cells are replicated in graphs D and E of Figures 1–13 and Supplementary Figures 2–14. Data for WT cells cultured with 0.1% PE21 are replicated in graphs D and E of Figure 3, Figure 7, Figure 8, Supplementary Figure 4, Supplementary Figure 8 and Supplementary Figure 11. Data for WT cells cultured with 50 μM R are replicated in graphs D and E of Figures 11–13, Supplementary Figure 13 and Supplementary Figure 14. (F) p Values for different pairs of survival curves of WT cells cultured in the presence of 0.1% PE21, 50 μM R, a mixture of 0.1% PE21 and 50 μM R, or in the absence of a PE and R (cells were subjected to ethanol-mock treatment) are shown. Survival curves shown in (D) were compared. The p values are displayed on a yellow or blue color background for the reasons described in the legend to Figure 1. Abbreviations: as in the legend to Figure 1.

MATERIALS AND METHODS

Yeast strains, media and growth conditions

The wild-type strain *Saccharomyces cerevisiae* BY4742 (*MATa his3D1 leu2D0 lys2D0 ura3D0*) and single-gene-deletion mutant strains in the BY4742 genetic background (all from Thermo Scientific/Open Biosystems) were grown in a synthetic minimal YNB medium (0.67% (w/v) Yeast Nitrogen Base without amino acids) initially containing 2% (w/v) glucose and supplemented with 20 mg/l histidine, 30 mg/l leucine, 30 mg/l lysine and 20 mg/l uracil. Cells were cultured at 30°C with rotational shaking at 200 rpm in Erlenmeyer flasks at a “flask volume/medium volume” ratio of 5:1.

Aging-delaying PEs

PE4 (an extract from the root and rhizome of *Cimicifuga racemosa*), PE5 (an extract from the root of *Valeriana officinalis L.*), PE6 (an extract from the whole plant of *Passiflora incarnata L.*), PE8 (an extract from the leaf of *Ginkgo biloba*), PE12 (an extract from the seed of *Apium graveolens L.*) and PE21 (an extract from the bark of *Salix alba*) were used at the final concentration of 0.1% (w/v), 0.3% (w/v), 0.5% (w/v) or 1.0% (w/v) [86]. A stock solution of each PE in ethanol was made on the day of adding this PE to cell cultures. For each PE, the stock solution was added to growth medium with 2% (w/v) glucose immediately following cell inoculation into the medium. In a culture supplemented with a PE, ethanol was used as a vehicle at the final concentration of 2.5% (v/v). In the same experiment, yeast cells were also subjected to ethanol-mock treatment by being cultured in growth medium initially containing 2% glucose and 2.5% (v/v) ethanol.

CLS assay

A sample of cells was taken from a culture at a certain day following cell inoculation and PE addition into the medium. A fraction of the sample was diluted to determine the total number of cells using a hemacytometer. Another fraction of the cell sample was diluted, and serial dilutions of cells were plated in duplicate onto YEP (1% (w/v) yeast extract, 2% (w/v) peptone) plates containing 2% (w/v) glucose as carbon source. After 2 d of incubation at 30°C, the number of colony forming units (CFU) per plate was counted. The number of CFU was defined as the number of viable cells in a sample. For each culture, the percentage of viable cells was calculated as follows: (number of viable cells per ml/total number of cells per ml) × 100. The percentage of viable cells in mid-logarithmic growth phase was set at 100%.

Statistical analysis

Statistical analysis was performed using Microsoft Excel's (2010) Analysis ToolPack-VBA. All data on cell

survival are presented as mean ± SEM. The *p* values for comparing the means of two groups using an unpaired two-tailed *t* test were calculated with the help of the GraphPad Prism 7 statistics software. The logrank test for comparing each pair of survival curves was performed with GraphPad Prism 7. Two survival curves were considered statistically different if the *p* value was less than 0.05.

Abbreviations

ATG, autophagy; AMPK, AMP-activated protein kinase; CFU, colony forming units; CI, combination index; CLS, chronological lifespan; CR, caloric restriction; HSA, highest single agent; IGF-1, insulin-like growth factor 1; PDTC, pyrrolidine dithiocarbamates; PEs, plant extracts; PKA, protein kinase A; PKH1/2, Pkb-activating kinase homologs 1 and 2; TCM, traditional Chinese medicine; Rim15, an anti-aging protein kinase; Sch9, a pro-aging protein kinase; SNF1, sucrose non-fermenting protein 1; TOR, target of rapamycin; TORC1, target of rapamycin complex 1.

ACKNOWLEDGMENTS

We are grateful to current and former members of the Titorenko laboratory for discussions. We acknowledge the Centre for Structural and Functional Genomics at Concordia University for outstanding services.

CONFLICTS OF INTEREST

The authors declare no conflicts of interest.

FUNDING

This study was supported by grants from the Natural Sciences and Engineering Research Council (NSERC) of Canada (RGPIN 2014-04482 and CRDPJ 515900 - 17), and Concordia University Chair Fund (CC0113). P.D. was supported by the Concordia University Graduate Fellowship Award. J.A.B.J. was supported by the Concordia University Merit Award.

REFERENCES

1. Yuan R, Lin Y. Traditional Chinese medicine: an approach to scientific proof and clinical validation. *Pharmacol Ther.* 2000; 86:191–98. [https://doi.org/10.1016/S0163-7258\(00\)00039-5](https://doi.org/10.1016/S0163-7258(00)00039-5).
2. Tang JL, Liu BY, Ma KW. Traditional Chinese medicine. *Lancet.* 2008; 372:1938–40. [https://doi.org/10.1016/S0140-6736\(08\)61354-9](https://doi.org/10.1016/S0140-6736(08)61354-9).
3. Xu Z. Modernization: one step at a time. *Nature.* 2011; 480:S90–92. <https://doi.org/10.1038/480S90a>. Erratum in: *Nature.* 2013; 495:270.

4. Hao C, Xiao PG. Network pharmacology: a Rosetta Stone for traditional Chinese medicine. *Drug Dev Res.* 2014; 75:299–312. <https://doi.org/10.1002/ddr.21214>.
5. Buriani A, Garcia-Bermejo ML, Bosisio E, Xu Q, Li H, Dong X, Simmonds MS, Carrara M, Tejedor N, Lucio-Cazana J, Hylands PJ. Omic techniques in systems biology approaches to traditional Chinese medicine research: present and future. *J Ethnopharmacol.* 2012; 140:535–44. <https://doi.org/10.1016/j.jep.2012.01.055>.
6. Uzuner H, Bauer R, Fan TP, Guo DA, Dias A, El-Nezami H, Efferth T, Williamson EM, Heinrich M, Robinson N, Hylands PJ, Hendry BM, Cheng YC, Xu Q. Traditional Chinese medicine research in the post-genomic era: good practice, priorities, challenges and opportunities. *J Ethnopharmacol.* 2012; 140:458–68. <https://doi.org/10.1016/j.jep.2012.02.028>.
7. Xue R, Fang Z, Zhang M, Yi Z, Wen C, Shi T. TCMID: traditional Chinese Medicine integrative database for herb molecular mechanism analysis. *Nucleic Acids Res.* 2013; 41:D1089–95. <https://doi.org/10.1093/nar/gks1100>.
8. Sánchez-Vidaña DI, Rajwani R, Wong MS. The use of omic technologies applied to traditional Chinese medicine research. *Evid Based Complement Alternat Med.* 2017; 2017:6359730. <https://doi.org/10.1155/2017/6359730>.
9. Hopkins AL. Network pharmacology. *Nat Biotechnol.* 2007; 25:1110–11. <https://doi.org/10.1038/nbt1007-1110>.
10. Li S, Zhang ZQ, Wu LJ, Zhang XG, Li YD, Wang YY. Understanding ZHENG in traditional Chinese medicine in the context of neuro-endocrine-immune network. *IET Syst Biol.* 2007; 1:51–60. <https://doi.org/10.1049/iet-syb:20060032>.
11. Li S, Zhang B. Traditional Chinese medicine network pharmacology: theory, methodology and application. *Chin J Nat Med.* 2013; 11:110–20. [https://doi.org/10.1016/S1875-5364\(13\)60037-0](https://doi.org/10.1016/S1875-5364(13)60037-0).
12. Tao W, Xu X, Wang X, Li B, Wang Y, Li Y, Yang L. Network pharmacology-based prediction of the active ingredients and potential targets of Chinese herbal Radix Curcumae formula for application to cardiovascular disease. *J Ethnopharmacol.* 2013; 145:1–10. <https://doi.org/10.1016/j.jep.2012.09.051>.
13. Liang X, Li H, Li S. A novel network pharmacology approach to analyse traditional herbal formulae: the Liu-Wei-Di-Huang pill as a case study. *Mol Biosyst.* 2014; 10:1014–22. <https://doi.org/10.1039/C3MB70507B>.
14. Tang F, Tang Q, Tian Y, Fan Q, Huang Y, Tan X. Network pharmacology-based prediction of the active ingredients and potential targets of Mahuang Fuzi Xixin decoction for application to allergic rhinitis. *J Ethnopharmacol.* 2015; 176:402–12. <https://doi.org/10.1016/j.jep.2015.10.040>.
15. Li S. Exploring traditional chinese medicine by a novel therapeutic concept of network target. *Chin J Integr Med.* 2016; 22:647–52. <https://doi.org/10.1007/s11655-016-2499-9>.
16. Fang J, Wang L, Wu T, Yang C, Gao L, Cai H, Liu J, Fang S, Chen Y, Tan W, Wang Q. Network pharmacology-based study on the mechanism of action for herbal medicines in Alzheimer treatment. *J Ethnopharmacol.* 2017; 196:281–92. <https://doi.org/10.1016/j.jep.2016.11.034>.
17. Zeng L, Yang K. Exploring the pharmacological mechanism of Yanghe Decoction on HER2-positive breast cancer by a network pharmacology approach. *J Ethnopharmacol.* 2017; 199:68–85. <https://doi.org/10.1016/j.jep.2017.01.045>.
18. Chen L, Cao Y, Zhang H, Lv D, Zhao Y, Liu Y, Ye G, Chai Y. Network pharmacology-based strategy for predicting active ingredients and potential targets of Yangxinshi tablet for treating heart failure. *J Ethnopharmacol.* 2018; 219:359–68. <https://doi.org/10.1016/j.jep.2017.12.011>.
19. Zuo H, Zhang Q, Su S, Chen Q, Yang F, Hu Y. A network pharmacology-based approach to analyse potential targets of traditional herbal formulas: an example of Yu Ping Feng decoction. *Sci Rep.* 2018; 8:11418. <https://doi.org/10.1038/s41598-018-29764-1>.
20. Ding F, Zhang Q, Ung CO, Wang Y, Han Y, Hu Y, Qi J. An analysis of chemical ingredients network of Chinese herbal formulae for the treatment of coronary heart disease. *PLoS One.* 2015; 10:e0116441. <https://doi.org/10.1371/journal.pone.0116441>.
21. Liang H, Ruan H, Ouyang Q, Lai L. Herb-target interaction network analysis helps to disclose molecular mechanism of traditional Chinese medicine. *Sci Rep.* 2016; 6:36767. <https://doi.org/10.1038/srep36767>.
22. Zhang Y, Mao X, Su J, Geng Y, Guo R, Tang S, Li J, Xiao X, Xu H, Yang H. A network pharmacology-based strategy deciphers the underlying molecular mechanisms of Qixuehe Capsule in the treatment of menstrual disorders. *Chin Med.* 2017; 12:23. <https://doi.org/10.1186/s13020-017-0145-x>.
23. Borisy AA, Elliott PJ, Hurst NW, Lee MS, Lehar J, Price ER, Serbedzija G, Zimmermann GR, Foley MA, Stockwell BR, Keith CT. Systematic discovery of multicomponent therapeutics. *Proc Natl Acad Sci U S A.* 2003; 100:7977–82. <https://doi.org/10.1073/pnas.1337088100>.
24. Csermely P, Agoston V, Pongor S. The efficiency of multi-target drugs: the network approach might help drug design. *Trends Pharmacol Sci.* 2005; 26:178–82. <https://doi.org/10.1016/j.tips.2005.02.007>.
25. Keith CT, Borisy AA, Stockwell BR. Multicomponent therapeutics for networked systems. *Nat Rev Drug Discov.* 2005; 4:71–78. <https://doi.org/10.1038/nrd1609>.
26. Smalley KS, Haass NK, Brafford PA, Lioni M, Flaherty KT, Herlyn M. Multiple signaling pathways must be targeted to overcome drug resistance in cell lines derived from melanoma metastases. *Mol Cancer Ther.* 2006; 5:1136–44. <https://doi.org/10.1158/1535-7163.MCT-06-0084>.
27. Kitano H. A robustness-based approach to systems-oriented drug design. *Nat Rev Drug Discov.* 2007; 6:202–10. <https://doi.org/10.1038/nrd2195>.

28. Zimmermann GR, Lehár J, Keith CT. Multi-target therapeutics: when the whole is greater than the sum of the parts. *Drug Discov Today*. 2007; 12:34–42. <https://doi.org/10.1016/j.drudis.2006.11.008>.
29. Lehár J, Stockwell BR, Giaever G, Nislow C. Combination chemical genetics. *Nat Chem Biol*. 2008; 4:674–81. <https://doi.org/10.1038/nchembio.120>.
30. Podolsky SH, Greene JA. Combination drugs—hype, harm, and hope. *N Engl J Med*. 2011; 365:488–91. <https://doi.org/10.1056/NEJMp1106161>.
31. Csermely P, Korcsmáros T, Kiss HJ, London G, Nussinov R. Structure and dynamics of molecular networks: a novel paradigm of drug discovery: a comprehensive review. *Pharmacol Ther*. 2013; 138:333–408. <https://doi.org/10.1016/j.pharmthera.2013.01.016>.
32. Baym M, Stone LK, Kishony R. Multidrug evolutionary strategies to reverse antibiotic resistance. *Science*. 2016; 351:aad3292. <https://doi.org/10.1126/science.aad3292>.
33. He B, Lu C, Zheng G, He X, Wang M, Chen G, Zhang G, Lu A. Combination therapeutics in complex diseases. *J Cell Mol Med*. 2016; 20:2231–40. <https://doi.org/10.1111/jcmm.12930>.
34. Lopez JS, Banerji U. Combine and conquer: challenges for targeted therapy combinations in early phase trials. *Nat Rev Clin Oncol*. 2017; 14:57–66. <https://doi.org/10.1038/nrclinonc.2016.96>.
35. Singh N, Yeh PJ. Suppressive drug combinations and their potential to combat antibiotic resistance. *J Antibiot (Tokyo)*. 2017; 70:1033–42. <https://doi.org/10.1038/ja.2017.102>.
36. Hao T, Wang Q, Zhao L, Wu D, Wang E, Sun J. Analyzing of molecular networks for human diseases and drug discovery. *Curr Top Med Chem*. 2018; 18:1007–14. <https://doi.org/10.2174/156802661866180813143408>.
37. Weiss A, Nowak-Sliwinska P. Current trends in multidrug optimization: an alley of future successful treatment of complex disorders. *SLAS Technol*. 2017; 22:254–75. <https://doi.org/10.1177/2472630316682338>.
38. Nelson HS. Advair: combination treatment with fluticasone propionate/salmeterol in the treatment of asthma. *J Allergy Clin Immunol*. 2001; 107:398–416. <https://doi.org/10.1067/mai.2001.112939>.
39. Glass G. Cardiovascular combinations. *Nat Rev Drug Discov*. 2004; 3:731–32. <https://doi.org/10.1038/nrd1501>.
40. Herrick TM, Million RP. Tapping the potential of fixed-dose combinations. *Nat Rev Drug Discov*. 2007; 6:513–14. <https://doi.org/10.1038/nrd2334>.
41. Pangalos MN, Schechter LE, Hurko O. Drug development for CNS disorders: strategies for balancing risk and reducing attrition. *Nat Rev Drug Discov*. 2007; 6:521–32. <https://doi.org/10.1038/nrd2094>.
42. Kummar S, Chen HX, Wright J, Holbeck S, Millin MD, Tomaszewski J, Zweibel J, Collins J, Doroshow JH. Utilizing targeted cancer therapeutic agents in combination: novel approaches and urgent requirements. *Nat Rev Drug Discov*. 2010; 9:843–56. <https://doi.org/10.1038/nrd3216>.
43. Humphrey RW, Brockway-Lunardi LM, Bonk DT, Dohoney KM, Doroshow JH, Meech SJ, Ratain MJ, Topalian SL, Pardoll DM. Opportunities and challenges in the development of experimental drug combinations for cancer. *J Natl Cancer Inst*. 2011; 103:1222–26. <https://doi.org/10.1093/jnci/djr246>.
44. Casado JL, Bañón S. Dutrebris (lamivudine and raltegravir) for use in combination with other antiretroviral products for the treatment of HIV-1 infection. *Expert Rev Clin Pharmacol*. 2015; 8:709–18. <https://doi.org/10.1586/17512433.2015.1090873>.
45. Horita N, Kaneko T. Role of combined indacaterol and glycopyrronium bromide (QVA149) for the treatment of COPD in Japan. *Int J Chron Obstruct Pulmon Dis*. 2015; 10:813–22. <https://doi.org/10.2147/COPD.S56067>.
46. Yang J, Tang H, Li Y, Zhong R, Wang T, Wong S, Xiao G, Xie Y. DIGRE: drug-induced genomic residual effect model for successful prediction of multidrug effects. *CPT Pharmacometrics Syst Pharmacol*. 2015; 4:e1. <https://doi.org/10.1002/psp4.1>.
47. Patel SJ, Kuten SA, Musick WL, Gaber AO, Monsour HP, Knight RJ. Combination drug products for HIV-A word of caution for the transplant clinician. *Am J Transplant*. 2016; 16:2479–82. <https://doi.org/10.1111/ajt.13826>.
48. Spitzer M, Robbins N, Wright GD. Combinatorial strategies for combating invasive fungal infections. *Virulence*. 2017; 8:169–85. <https://doi.org/10.1080/21505594.2016.1196300>.
49. Yin Z, Deng Z, Zhao W, Cao Z. Searching synergistic dose combinations for anticancer drugs. *Front Pharmacol*. 2018; 9:535. <https://doi.org/10.3389/fphar.2018.00535>.
50. Lehár J, Zimmermann GR, Krueger AS, Molnar RA, Ledell JT, Heilbut AM, Short GF 3rd, Giusti LC, Nolan GP, Magid OA, Lee MS, Borisy AA, Stockwell BR, Keith CT. Chemical combination effects predict connectivity in biological systems. *Mol Syst Biol*. 2007; 3:80. <https://doi.org/10.1038/msb4100116>.
51. Yeh P, Kishony R. Networks from drug-drug surfaces. *Mol Syst Biol*. 2007; 3:85. <https://doi.org/10.1038/msb4100133>.
52. Chou TC. Drug combination studies and their synergy quantification using the Chou-Talalay method. *Cancer Res*. 2010; 70:440–46. <https://doi.org/10.1158/0008-5472.CAN-09-1947>.
53. Tallarida RJ. Quantitative methods for assessing drug synergism. *Genes Cancer*. 2011; 2:1003–08. <https://doi.org/10.1177/1947601912440575>.
54. Zou J, Ji P, Zhao YL, Li LL, Wei YQ, Chen YZ, Yang SY. Neighbor communities in drug combination networks characterize synergistic effect. *Mol Biosyst*. 2012; 8:3185–96. <https://doi.org/10.1039/c2mb25267h>.
55. Bansal M, Yang J, Karan C, Menden MP, Costello JC, Tang H, Xiao G, Li Y, Allen J, Zhong R, Chen B, Kim

- M, Wang T, et al, and NCI-DREAM Community. A community computational challenge to predict the activity of pairs of compounds. *Nat Biotechnol.* 2014; 32:1213–22. <https://doi.org/10.1038/nbt.3052>.
56. Foucquier J, Guedj M. Analysis of drug combinations: current methodological landscape. *Pharmacol Res Perspect.* 2015; 3:e00149. <https://doi.org/10.1002/prp2.149>.
57. Yadav B, Wennerberg K, Aittokallio T, Tang J. Searching for drug synergy in complex dose-response landscapes using an interaction potency Model. *Comput Struct Biotechnol J.* 2015; 13:504–13. <https://doi.org/10.1016/j.csbj.2015.09.001>. Erratum in: Corrigendum to “Searching for drug synergy in complex dose-response landscapes using an interaction potency model” [Comput. Struct. Biotechnol. J. 13 (2015) 504–513]. [Comput Struct Biotechnol J. 2017].
58. Li X, Qin G, Yang Q, Chen L, Xie L. Biomolecular network-based synergistic drug combination discovery. *Biomed Res Int.* 2016; 2016:8518945. <https://doi.org/10.1155/2016/8518945>.
59. Harman D. The aging process: major risk factor for disease and death. *Proc Natl Acad Sci U S A.* 1991; 88:5360–63. <https://doi.org/10.1073/pnas.88.12.5360>.
60. Blagosklonny MV. Validation of anti-aging drugs by treating age-related diseases. *Aging (Albany NY).* 2009; 1:281–88. <https://doi.org/10.1863/aging.100034>.
61. Niccoli T, Partridge L. Ageing as a risk factor for disease. *Curr Biol.* 2012; 22:R741–52. <https://doi.org/10.1016/j.cub.2012.07.024>.
62. Kaeberlein M. Longevity and aging. *F1000Prime Rep.* 2013; 5:5. <https://doi.org/10.12703/P5-5>.
63. Kaeberlein M. The biology of aging: citizen scientists and their pets as a bridge between research on model organisms and human subjects. *Vet Pathol.* 2016; 53:291–98. <https://doi.org/10.1177/0300985815591082>.
64. de Cabo R, Carmona-Gutierrez D, Bernier M, Hall MN, Madeo F. The search for antiaging interventions: from elixirs to fasting regimens. *Cell.* 2014; 157:1515–26. <https://doi.org/10.1016/j.cell.2014.05.031>.
65. Kennedy BK, Berger SL, Brunet A, Campisi J, Cuervo AM, Epel ES, Franceschi C, Lithgow GJ, Morimoto RI, Pessin JE, Rando TA, Richardson A, Schadt EE, et al. Geroscience: linking aging to chronic disease. *Cell.* 2014; 159:709–13. <https://doi.org/10.1016/j.cell.2014.10.039>.
66. Longo VD, Antebi A, Bartke A, Barzilai N, Brown-Borg HM, Caruso C, Curiel TJ, de Cabo R, Franceschi C, Gems D, Ingram DK, Johnson TE, Kennedy BK, et al. Interventions to slow aging in humans: are we ready? *Aging Cell.* 2015; 14:497–510. <https://doi.org/10.1111/acel.12338>.
67. Fontana L, Partridge L, Longo VD. Extending healthy life span—from yeast to humans. *Science.* 2010; 328:321–26. <https://doi.org/10.1126/science.1172539>.
68. López-Otín C, Blasco MA, Partridge L, Serrano M, Kroemer G. The hallmarks of aging. *Cell.* 2013; 153:1194–217. <https://doi.org/10.1016/j.cell.2013.05.039>.
69. Carvalhal Marques F, Volovik Y, Cohen E. The roles of cellular and organismal aging in the development of late-onset maladies. *Annu Rev Pathol.* 2015; 10:1–23. <https://doi.org/10.1146/annurev-pathol-012414-040508>.
70. Fontana L, Partridge L. Promoting health and longevity through diet: from model organisms to humans. *Cell.* 2015; 161:106–18. <https://doi.org/10.1016/j.cell.2015.02.020>.
71. Mazucanti CH, Cabral-Costa JV, Vasconcelos AR, Andreotti DZ, Scavone C, Kawamoto EM. Longevity pathways (mTOR, SIRT, Insulin/IGF-1) as key modulatory targets on aging and neurodegeneration. *Curr Top Med Chem.* 2015; 15:2116–38. <https://doi.org/10.2174/1568026615666150610125715>.
72. Burkewitz K, Weir HJ, Mair WB. AMPK as a Pro-longevity Target. *Exp Suppl.* 2016; 107:227–56.
73. Pan H, Finkel T. Key proteins and pathways that regulate lifespan. *J Biol Chem.* 2017; 292:6452–60. <https://doi.org/10.1074/jbc.R116.771915>.
74. Aliper A, Belikov AV, Garazha A, Jellen L, Artemov A, Suntsova M, Ivanova A, Venkova L, Borisov N, Buzdin A, Mamoshina P, Putin E, Swick AG, et al. In search for geroprotectors: in silico screening and *in vitro* validation of signalome-level mimetics of young healthy state. *Aging (Albany NY).* 2016; 8:2127–52. <https://doi.org/10.1863/aging.101047>.
75. Moskalev A, Chernyagina E, Tsvetkov V, Fedintsev A, Shaposhnikov M, Krut'ko V, Zhavoronkov A, Kennedy BK. Developing criteria for evaluation of geroprotectors as a key stage toward translation to the clinic. *Aging Cell.* 2016; 15:407–15. <https://doi.org/10.1111/acel.12463>.
76. Blagosklonny MV. From rapalogs to anti-aging formula. *Oncotarget.* 2017; 8:35492–507. <https://doi.org/10.1863/oncotarget.18033>.
77. Ladiges W, Liggitt D. Testing drug combinations to slow aging. *Pathobiol Aging Age Relat Dis.* 2017; 8:1407203. <https://doi.org/10.1080/20010001.2017.1407203>.
78. Blagosklonny MV. Koschei the immortal and anti-aging drugs. *Cell Death Dis.* 2014; 5:e1552. <https://doi.org/10.1038/cddis.2014.520>.
79. Strong R, Miller RA, Antebi A, Astle CM, Bogue M, Denzel MS, Fernandez E, Flurkey K, Hamilton KL, Lamming DW, Javors MA, de Magalhães JP, Martinez PA, et al. Longer lifespan in male mice treated with a weakly estrogenic agonist, an antioxidant, an α -glucosidase inhibitor or a Nrf2-inducer. *Aging Cell.* 2016; 15:872–84. <https://doi.org/10.1111/acel.12496>.
80. Weiss R, Fernandez E, Liu Y, Strong R, Salmon AB. Metformin reduces glucose intolerance caused by rapamycin treatment in genetically heterogeneous female mice. *Aging (Albany NY).* 2018; 10:386–401. <https://doi.org/10.1863/aging.101401>.
81. Danilov A, Shaposhnikov M, Plyusnina E, Kogan V, Fedichev P, Moskalev A. Selective anticancer agents

- suppress aging in *Drosophila*. *Oncotarget*. 2013; 4:1507–26. <https://doi.org/10.18632/oncotarget.1272>.
82. Snell TW, Johnston RK, Rabeneck B, Zipperer C, Teat S. Joint inhibition of TOR and JNK pathways interacts to extend the lifespan of *Brachionus manjavacas* (Rotifera). *Exp Gerontol*. 2014; 52:55–69. <https://doi.org/10.1016/j.exger.2014.01.022>.
83. Admasu TD, Chaithanya Batchu K, Barardo D, Ng LF, Lam VY, Xiao L, Cazenave-Gassiot A, Wenk MR, Tolwinski NS, Gruber J. Drug synergy slows aging and improves healthspan through IGF and SREBP lipid signaling. *Dev Cell*. 2018; 47:67–79.e5. <https://doi.org/10.1016/j.devcel.2018.09.001>.
84. Huang X, Liu J, Withers BR, Samide AJ, Leggas M, Dickson RC. Reducing signs of aging and increasing lifespan by drug synergy. *Aging Cell*. 2013; 12:652–60. <https://doi.org/10.1111/acel.12090>.
85. Huang X, Leggas M, Dickson RC. Drug synergy drives conserved pathways to increase fission yeast lifespan. *PLoS One*. 2015; 10:e0121877. <https://doi.org/10.1371/journal.pone.0121877>. Erratum in: Correction: Drug synergy drives conserved pathways to increase fission yeast lifespan. [PLOS One. 2015].
86. Lutchman V, Medkour Y, Samson E, Arlia-Ciommo A, Dakik P, Cortes B, Feldman R, Mohtashami S, McAuley M, Chancharoen M, Rukundo B, Simard É, Titorenko VI. Discovery of plant extracts that greatly delay yeast chronological aging and have different effects on longevity-defining cellular processes. *Oncotarget*. 2016; 7:16542–66. <https://doi.org/10.18632/oncotarget.7665>.
87. Lutchman V, Dakik P, McAuley M, Cortes B, Ferraye G, Gontmacher L, Graziano D, Moukhariq FZ, Simard É, Titorenko VI. Six plant extracts delay yeast chronological aging through different signaling pathways. *Oncotarget*. 2016; 7:50845–63. <https://doi.org/10.18632/oncotarget.10689>.
88. Eisenberg T, Knauer H, Schauer A, Büttner S, Ruckenstein C, Carmona-Gutierrez D, Ring J, Schroeder S, Magnes C, Antonacci L, Fussi H, Deszcz L, Hartl R, et al. Induction of autophagy by spermidine promotes longevity. *Nat Cell Biol*. 2009; 11:1305–14. <https://doi.org/10.1038/ncb1975>.
89. Morselli E, Galluzzi L, Kepp O, Criollo A, Maiuri MC, Tavernarakis N, Madeo F, Kroemer G. Autophagy mediates pharmacological lifespan extension by spermidine and resveratrol. *Aging (Albany NY)*. 2009; 1:961–70. <https://doi.org/10.18632/aging.100110>.
90. Goldberg AA, Richard VR, Kyryakov P, Bourque SD, Beach A, Burstein MT, Glebov A, Koupaki O, Boukh-Viner T, Gregg C, Juneau M, English AM, Thomas DY, Titorenko VI. Chemical genetic screen identifies lithocholic acid as an anti-aging compound that extends yeast chronological life span in a TOR-independent manner, by modulating housekeeping longevity assurance processes. *Aging (Albany NY)*. 2010; 2:393–414. <https://doi.org/10.18632/aging.100168>.
91. Kaeberlein M. Lessons on longevity from budding yeast. *Nature*. 2010; 464:513–19. <https://doi.org/10.1038/nature08981>. Erratum in: *Nature*. 2010; 464:1390.
92. Minois N, Carmona-Gutierrez D, Madeo F. Polyamines in aging and disease. *Aging (Albany NY)*. 2011; 3:716–32. <https://doi.org/10.18632/aging.100361>.
93. Váchová L, Cáp M, Palková Z. Yeast colonies: a model for studies of aging, environmental adaptation, and longevity. *Oxid Med Cell Longev*. 2012; 2012:601836. <https://doi.org/10.1155/2012/601836>.
94. Hubbard BP, Sinclair DA. Small molecule SIRT1 activators for the treatment of aging and age-related diseases. *Trends Pharmacol Sci*. 2014; 35:146–54. <https://doi.org/10.1016/j.tips.2013.12.004>.
95. Leonov A, Arlia-Ciommo A, Piano A, Svistkova V, Lutchman V, Medkour Y, Titorenko VI. Longevity extension by phytochemicals. *Molecules*. 2015; 20:6544–72. <https://doi.org/10.3390/molecules20046544>.
96. Longo VD, Shadel GS, Kaeberlein M, Kennedy B. Replicative and chronological aging in *Saccharomyces cerevisiae*. *Cell Metab*. 2012; 16:18–31. <https://doi.org/10.1016/j.cmet.2012.06.002>.
97. Arlia-Ciommo A, Leonov A, Piano A, Svistkova V, Titorenko VI. Cell-autonomous mechanisms of chronological aging in the yeast *Saccharomyces cerevisiae*. *Microb Cell*. 2014; 1:163–78. <https://doi.org/10.15698/mic2014.06.152>.
98. Garay E, Campos SE, González de la Cruz J, Gaspar AP, Jinich A, Deluna A. High-resolution profiling of stationary-phase survival reveals yeast longevity factors and their genetic interactions. *PLoS Genet*. 2014; 10:e1004168. <https://doi.org/10.1371/journal.pgen.1004168>.
99. Madeo F, Carmona-Gutierrez D, Kepp O, Kroemer G. Spermidine delays aging in humans. *Aging (Albany NY)*. 2018; 10:2209–11. <https://doi.org/10.18632/aging.101517>.
100. Madeo F, Eisenberg T, Pietrocola F, Kroemer G. Spermidine in health and disease. *Science*. 2018; 359. <https://doi.org/10.1126/science.aan2788>.
101. Strynatka KA, Gurrola-Gal MC, Berman JN, McMaster CR. How surrogate and chemical genetics in model organisms can suggest therapies for human genetic diseases. *Genetics*. 2018; 208:833–51. <https://doi.org/10.1534/genetics.117.300124>.
102. Zimmermann A, Hofer S, Pendl T, Kainz K, Madeo F, Carmona-Gutierrez D. Yeast as a tool to identify anti-aging compounds. *FEMS Yeast Res*. 2018; 18:foy020. <https://doi.org/10.1093/femsyr/foy020>.
103. Fabrizio P, Pozza F, Pletcher SD, Gendron CM, Longo VD. Regulation of longevity and stress resistance by Sch9 in yeast. *Science*. 2001; 292:288–90. <https://doi.org/10.1126/science.1059497>.
104. Wei M, Fabrizio P, Hu J, Ge H, Cheng C, Li L, Longo VD. Life span extension by calorie restriction depends on Rim15 and transcription factors downstream of

- Ras/PKA, Tor, and Sch9. *PLoS Genet.* 2008; 4:e13. <https://doi.org/10.1371/journal.pgen.0040013>.
105. De Virgilio C. The essence of yeast quiescence. *FEMS Microbiol Rev.* 2012; 36:306–39. <https://doi.org/10.1111/j.1574-6976.2011.00287.x>.
106. Conrad M, Schothorst J, Kankipati HN, Van Zeebroeck G, Rubio-Texeira M, Thevelein JM. Nutrient sensing and signaling in the yeast *Saccharomyces cerevisiae*. *FEMS Microbiol Rev.* 2014; 38:254–99. <https://doi.org/10.1111/1574-6976.12065>.
107. Swinnen E, Ghillebert R, Wilms T, Winderickx J. Molecular mechanisms linking the evolutionary conserved TORC1-Sch9 nutrient signalling branch to lifespan regulation in *Saccharomyces cerevisiae*. *FEMS Yeast Res.* 2014; 14:17–32. <https://doi.org/10.1111/1567-1364.12097>.
108. Kapahi P, Chen D, Rogers AN, Katewa SD, Li PW, Thomas EL, Kockel L. With TOR, less is more: a key role for the conserved nutrient-sensing TOR pathway in aging. *Cell Metab.* 2010; 11:453–65. <https://doi.org/10.1016/j.cmet.2010.05.001>.
109. Smets B, Ghillebert R, De Snijder P, Bindt M, Swinnen E, De Virgilio C, Winderickx J. Life in the midst of scarcity: adaptations to nutrient availability in *Saccharomyces cerevisiae*. *Curr Genet.* 2010; 56:1–32. <https://doi.org/10.1007/s00294-009-0287-1>.
110. Titorenko VI, Terlecky SR. Peroxisome metabolism and cellular aging. *Traffic.* 2011; 12:252–59. <https://doi.org/10.1111/j.1600-0854.2010.01144.x>.
111. Broach JR. Nutritional control of growth and development in yeast. *Genetics.* 2012; 192:73–105. <https://doi.org/10.1534/genetics.111.135731>.
112. Kyryakov P, Beach A, Richard VR, Burstein MT, Leonov A, Levy S, Titorenko VI. Caloric restriction extends yeast chronological lifespan by altering a pattern of age-related changes in trehalose concentration. *Front Physiol.* 2012; 3:256. <https://doi.org/10.3389/fphys.2012.00256>.
113. Leonov A, Titorenko VI. A network of interorganellar communications underlies cellular aging. *IUBMB Life.* 2013; 65:665–74. <https://doi.org/10.1002/iub.1183>.
114. Engelberg D, Perlman R, Levitzki A. Transmembrane signaling in *Saccharomyces cerevisiae* as a model for signaling in metazoans: state of the art after 25 years. *Cell Signal.* 2014; 26:2865–78. <https://doi.org/10.1016/j.cellsig.2014.09.003>.
115. Rødkaer SV, Faergeman NJ. Glucose- and nitrogen sensing and regulatory mechanisms in *Saccharomyces cerevisiae*. *FEMS Yeast Res.* 2014; 14:683–96. <https://doi.org/10.1111/1567-1364.12157>.
116. Lee D, Hwang W, Artan M, Jeong DE, Lee SJ. Effects of nutritional components on aging. *Aging Cell.* 2015; 14:8–16. <https://doi.org/10.1111/acel.12277>.
117. Teixeira V, Costa V. Unraveling the role of the Target of Rapamycin signaling in sphingolipid metabolism. *Prog Lipid Res.* 2016; 61:109–33. <https://doi.org/10.1016/j.plipres.2015.11.001>.
118. Park SJ, Ahmad F, Philp A, Baar K, Williams T, Luo H, Ke H, Rehmann H, Taussig R, Brown AL, Kim MK, Beaven MA, Burgin AB, et al. Resveratrol ameliorates aging-related metabolic phenotypes by inhibiting cAMP phosphodiesterases. *Cell.* 2012; 148:421–33. <https://doi.org/10.1016/j.cell.2012.01.017>.
119. Sajish M, Schimmel P. A human tRNA synthetase is a potent PARP1-activating effector target for resveratrol. *Nature.* 2015; 519:370–73. <https://doi.org/10.1038/nature14028>.
120. Berenbaum MC. What is synergy? *Pharmacol Rev.* 1989; 41:93–141.
121. Slinker BK. The statistics of synergism. *J Mol Cell Cardiol.* 1998; 30:723–31. <https://doi.org/10.1006/jmcc.1998.0655>.
122. Nieuwenhuis S, Forstmann BU, Wagenaars EJ. Erroneous analyses of interactions in neuroscience: a problem of significance. *Nat Neurosci.* 2011; 14:1105–07. <https://doi.org/10.1038/nn.2886>.
123. Geary N. Understanding synergy. *Am J Physiol Endocrinol Metab.* 2013; 304:E237–53. <https://doi.org/10.1152/ajpendo.00308.2012>.